POLITECNICO DI TORINO

Master's Degree in Energy And Nuclear Engineering

Master’s Degree Thesis

Estimation of the potential of Power-to-Power systems in Pantelleria

Supervisor:

Prof. Massimo Santarelli

Advisor:

PhD. Domenico Ferrero

PhD. Paolo Marocco

Candidate:

Chiara Bergamin

Academic Year 2020-2021

A papà che mi manca ogni giorno

A mamma e Andrea per il loro amore costante

Abstract

Nowadays, the climate change threat represents the biggest challenge. The main cause is the emission of greenhouse gases (GHG), which are strictly related to fossil fuels exploitation. It is necessary to reassess the future scenarios in a sustainable way, where the use of renewable energy sources (RES) represents the pivotal point of the energy transition. The intermittent nature of RES requires a different strategy when compared to fossils resources. Energy storage systems represent the main solution to match energy consumption with production. In this framework, hydrogen storage represents one of the most valuable options. The hydrogen, obtained from water electrolysis, involves electricity from RES. In this case, hydrogen is a carbon-neutral energy carrier that can be used both as an end-use fuel, in the transport sector, and converted into electricity. The system configuration that exploits the RES linked to hydrogen storage is called Power-to-Power (P2P) system. It is a promising technology especially in isolated areas, like islands, that rely on fossil fuels and are not connected to the grid.

In this work, the case of Pantelleria, an island in Italy, is carried out. This analysis wants to demonstrate if the P2P configuration can be environmentally and economically sustainable. In particular, if the system studied can supply both the residential load and the public transport demand. The work is developed starting from the study of the current energy configuration of the island. Then the residential load and public transportation load are evaluated. The RES production, represented by solar and wind sources, is estimated with the meteorological data extracted from PVGIS. These data have been used as input vectors in a techno-economic optimization tool able to minimize the LCOE. An economic analysis is conducted to compare different scenarios and estimate which is the most advantageous. Finally, an environmental analysis is performed, in particular the avoided CO_2 emissions are evaluated.

Acronyms

CCS Carbon Capture and Storage

CCU Carbon Capture and Utilization

FC Fuel Cell

GHG Greenhouse Gases

P2P Power-to-Power

P2G Power-to-Gas

PV Photovoltaic

RES Renewable Energy Sources

TMY Typical Meteorological Year

PSO Particle Swarm Optimization

LPSP Loss of Power Supply Probability

LCOE Levelized Cost of Energy

LCOH Levelized Cost of Hydrogen

EMS Energy Management Strategy

SOC State Of Charge

LOH Level Of Hydrogen

Summary

CHAPTER 1

INTRODUCTION

1.1 General Background

The reconsideration of fossil fuels dependency in favour of the exploitation of renewable energy sources is the main objective of the global energy transition. This shift is driven by the growing concern about the consequences of climate change. Nevertheless, the constant rise in fossil fuels price encourages this change.

During the United Nations Climate Change Conference, held in Paris in 2015, an agreement was negotiated in which was established that the climate crisis needs to be solved globally. Basically, the major goal to be achieved is *«holding the increase in the global average temperature to well below 2°C above pre-industrial levels and pursuing efforts to limit the temperature increase to 1.5°C above pre-industrial levels, recognizing that this would significantly reduce the risks and impacts of climate change»* (1).

According to the *"Special Report on Global warming of 1.5°C"* (2) published by IPCC, anthropogenic emissions are one of the main sources of changes in the climate system, but these emissions alone do not cause global warming of 1.5°C. This report clarifies that, even if the 1.5°C limit is respected, climate-related risks are projected to increase. This is the reason why further efforts are required in a sustainable direction. In this respect, the worst effects of climate change can be limited with a drastic reduction of greenhouse gases, especially carbon dioxide (CO_2). The largest source of GHG emissions is represented by the production and use of energy. **Fig. 1** shows the CO_2 emissions considering different sectors.

In (2) is developed a framework of global warming impacts of 1.5°C above pre-industrial levels. In the simulated pathways the global net CO_2 emissions, from 2010 levels by 2030, decrease by about 45% and reach net zero around 2050. The increase to 1.5°C or, in the worst case, to 2°C, in the global warming, leads to an increase of:

- mean temperature in most land and ocean regions, with a special focus on the most inhabited regions.

- heavy precipitation in several regions, and drought events and precipitation deficits in some regions.

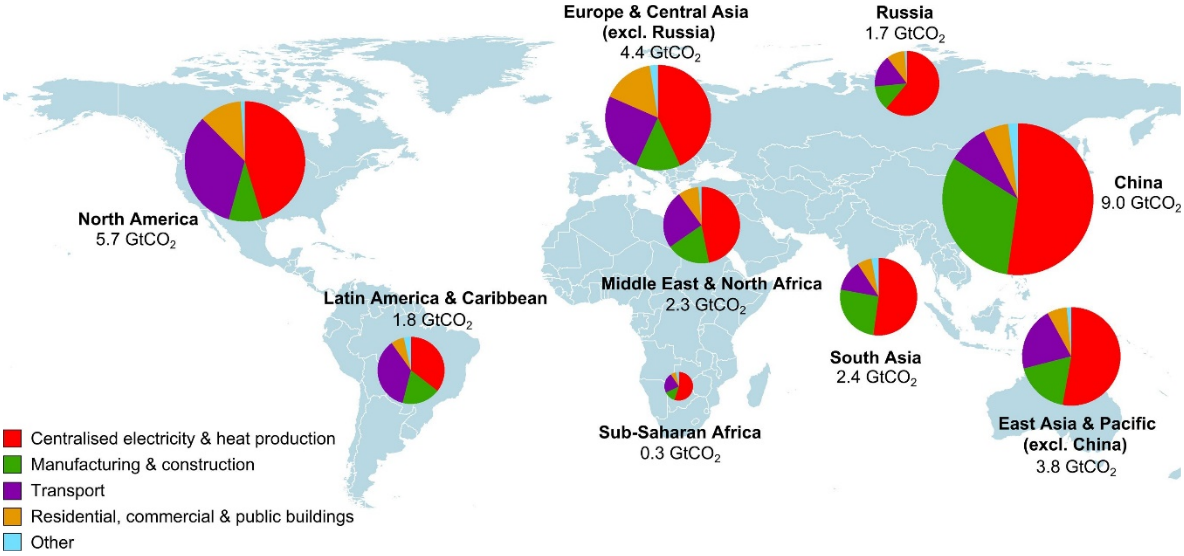

Fig. 1 *Global CO_2 emissions from fuel combustion in 2014 (3)*

According to the annual analysis carried on by the International Energy Agency (4), the Covid-19 pandemic has had a strong impact on the energy sector and on the energy transition. It is impossible to forecast how long the health emergency will last. This introduces uncertainty for the future of the energy sector, especially because it is strictly linked to the economy that is facing a global crisis. A strategic vision from governments is required to guide people towards a green future. In this context, the European Commission sets out initiatives to promote climate neutrality by 2050 in the *"European Green Deal"* (5). The policy areas are summarized in **Fig. 2**.

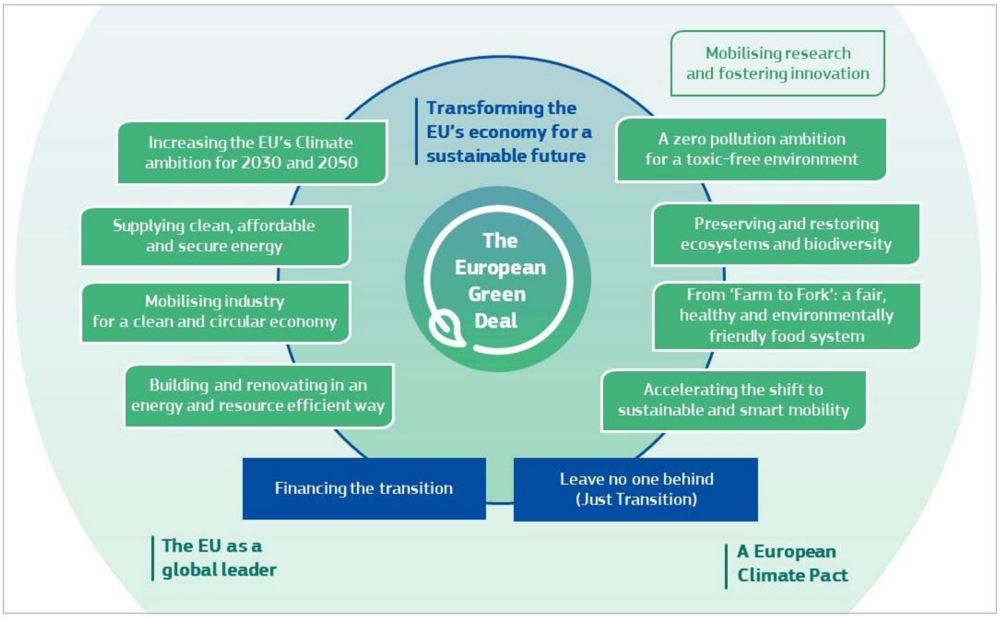

Fig. 2 Policy areas of European Green Deal (5)

In the energy transition, electricity plays a key role. Electricity demand rise and wealth growth, go hand in hand. Consequently, electricity generation needs decarbonization to reduce emissions. This goal can be achieved by exploiting renewable energy sources with the help of storage technologies ever more efficient. In fact, the latter, guarantee flexible operation of power systems. Solar leads among all the renewable sources, in particular solar photovoltaic has lowered the cost of electricity thanks to supportive policies and maturing technologies. The solar source, followed by onshore and offshore wind sources, are the main drivers in the growth of renewables exploitation (4).

In the framework of climate change mitigation, also carbon capture and storage is an interesting process to produce electricity from the existing fossil fuel power plants, cutting the emissions. The captured CO_2 can be seen as a resource in the production of synthetic fuels, joined by hydrogen, or used as an industrial feedstock. This process is called carbon capture and utilization. (3)

It has become clear that climate neutrality must be supported by net-zero greenhouse gases emissions, therefore it is necessary to find ways to take full advantage of renewables. Hydrogen can maximize their utilization enabling a decarbonization pathway. It has multiple applications: from end-use fuel to a feedstock to produce carbon-neutral hydrocarbons, but it can be used as a carrier of chemical storage of electricity (6).

According to the *"World Energy Outlook"* (7) published in 2019, the least-cost way to provide universal electricity access is a combination of on-grid, mini-grid and stand-alone systems. In this way, it is possible to reach remote areas.

1.2 Renewable Energy in Statistics

According to the *"World Energy Transitions Outlook: 1.5°C Pathway"* (8), the annual renewable power capacity installation, as well as the share of renewable energy in electricity, have shown a growing from 2013 and 2020. This is the result of the continuous decline of the cost of renewable energy, in particular solar PV, that now can compete with the cost of fossil-fuel-fired power generation. This is demonstrated by the global weighted average levelised cost of energy (LCOE) of utility-scale solar PV, it has fallen from 0.381 USD/kWh to 0.057 USD/kWh, between 2010 and 2020, while the actual cost of fossil-fuel-fired power generation varies by in an estimated range between 0.055 USD/kWh and 0.148 USD/kWh, depending on the country and fuel.

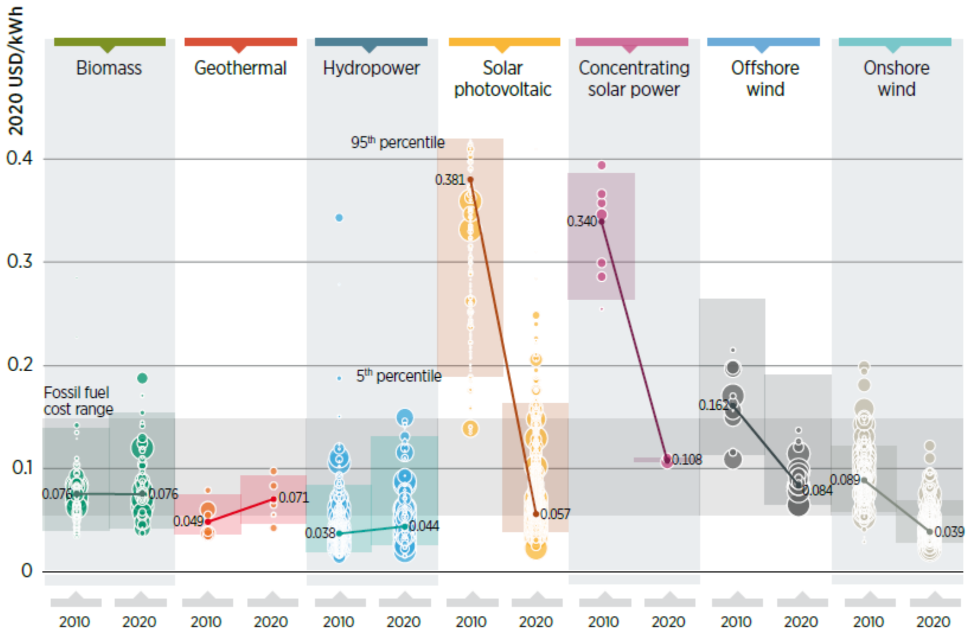

Fig. 3 Global LCOE of newly commissioned utility-scale renewable power generation technologies, 2010 and 2020 (8)

Going back to the annual capacity installation, it has increased globally with an addition of more than 260 GW of new renewable capacity in 2020. Despite the Covid-19 pandemic, renewable capacity has experienced a growth with the consequent decline of non-renewable capacity, showing the potential opportunities of RES. In 2020, 127 GW of solar PV power were installed, while the wind power reached a total of 111 GW. As a consequence of this growth, also the share of renewables has recorded an increment that is shown in **Fig. 4**.

In this framework of growth, there is no shortage of complications due to higher system requirements, which need a wide range of innovations, like battery storage and smart grids. Renewables represent an opportunity for investors, thanks to the rapid growth of technologies.

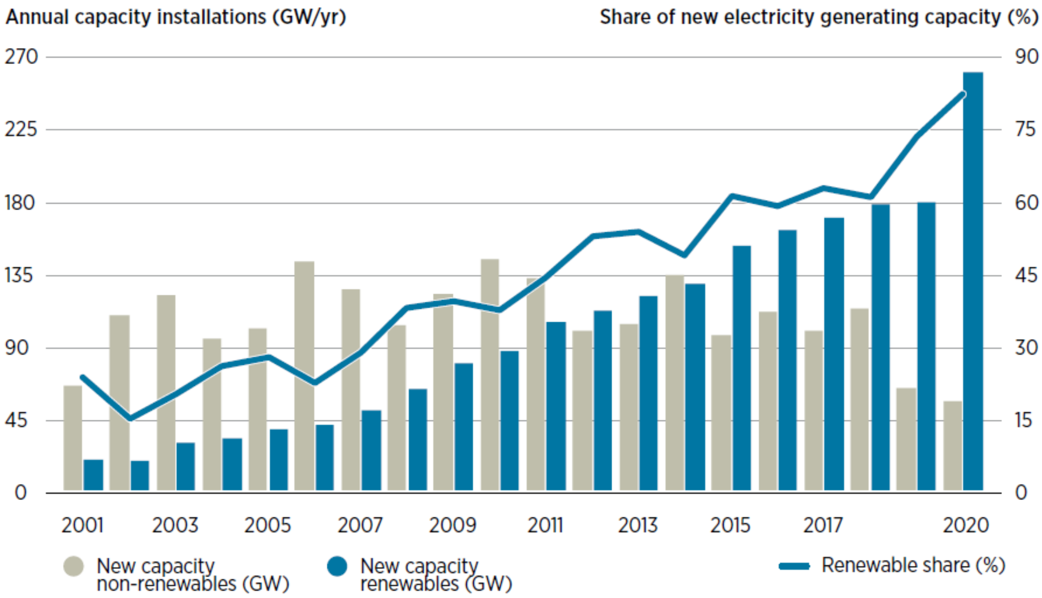

Fig. 4 Share of new electricity capacity, 2001-2020 (8)

At European level, thanks to binding targets among the EU Member States, aiming to the promotion to use energy from renewable sources, the share of renewables in gross final energy consumption was 19.7% in 2019, compared with 9.6% in 2004 (9). The EU has fixed the 20% share target of its gross final energy consumption from renewable sources by 2020.

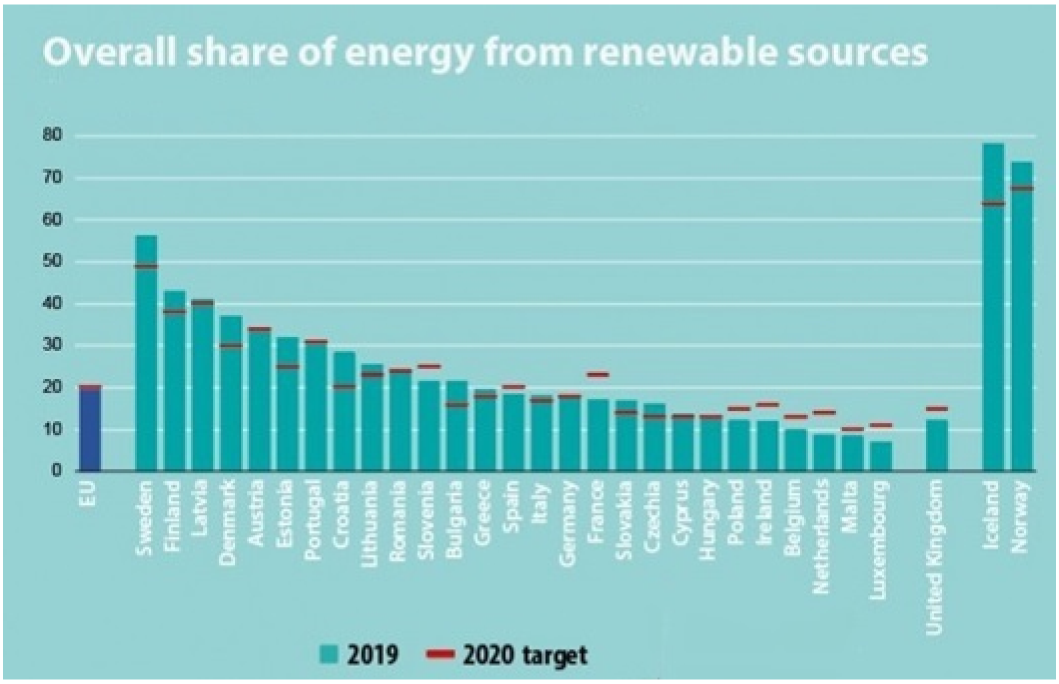

Fig. 5 Percentage of gross final energy consumption in 2019 (9)

Considering the installed electrical capacity, in 2019, the EU recorded a growth in the share of wind of 17.6% and in the share of solar PV of 12.5%, with a consequent decreasing share of fossil fuels up to 41.9% (10), as reported in **Fig. 6**.

	2000	2001	2002	2003	2004	2005	2006	2016	2017	2018	2019
Total capacity	613 221	620 965	634 362	637 307	657 278	675 657	693 041	895 755	907 418	930 757	947 338
Combustible fuels	340 088	342 896	348 549	346 552	359 149	370 324	379 790	401 885	398 249	405 743	396 936
Hydro	134 729	135 058	135 438	135 861	137 713	139 271	139 516	149 838	150 481	150 501	150 912
Pure hydro power	95 932	96 100	96 423	97 127	98 019	98 361	98 168	104 031	104 446	104 643	105 033
Mixed hydro power	18 321	18 346	18 331	18 381	18 758	19 246	19 690	22 804	23 248	23 210	23 231
Pumped hydro power	20 476	20 612	20 684	20 353	20 936	21 665	21 659	23 003	22 787	22 648	22 648
Geothermal	604	587	682	723	658	686	697	841	848	861	866
Wind	12 297	16 845	22 603	27 253	33 156	38 773	45 612	137 998	148 920	157 172	167 140
Solar	175	272	355	588	1 295	2 268	3 224	91 498	96 231	104 062	120 393
Solar thermal	0	0	0	0	0	0	11	2 306	2 306	2 306	2 315
Solar photovoltaic	175	272	355	588	1 295	2 268	3 213	89 192	93 925	101 756	118 077
Tide, wave, ocean	213	215	218	219	218	216	215	225	224	223	219
Nuclear	124 851	124 882	126 297	125 416	124 555	123 142	122 837	112 554	111 524	111 240	109 954
Other sources	263	210	220	695	534	977	1 149	917	942	955	918

Fig. 6 Maximum electrical capacity 2000-2019 (10)

In 2019, the share of renewable energy sources stood at 34% of gross electricity consumption, where hydro and wind power are the main sources exploited, followed by solar power (9). The latter has experienced the fastest growth thanks to the support from governments and a drop in costs. **Fig. 7** shows the electricity consumption in the EU from renewable sources in 2019.

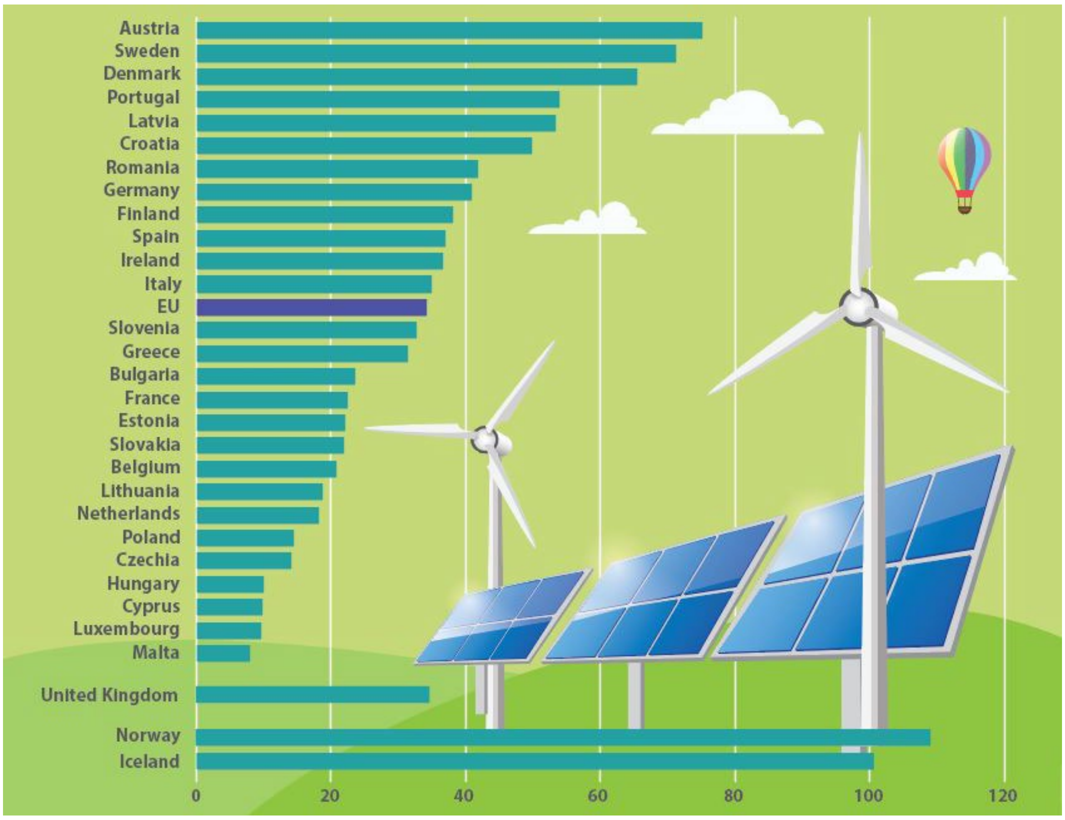

Fig. 7 Percentage, from renewable sources, of gross final energy consumption in 2019 (9)

1.3 Thesis Objectives

Off-grid islands and isolated sites, that usually rely on fossil fuels for electricity generation purposes, are attractive locations for renewable energy sources exploitation to let them to be self-sufficient and economically sustainable. In fact, the use of fossil fuels makes power generation expensive. The remote areas represent the best candidate for the utilization of renewables, but the issue of intermittency has to be solved. The most viable and reliable option is represented by power-to-power systems (11). The aim of them is to convert the electricity produced by RES into liquids, gases, or fuels and back from those into electricity. They can operate in two different modes: charging mode, in which electricity is consumed, and discharging mode, where electricity is produced (12).

The island of Pantelleria, in Italy, represents an attractive location to analyse the potential of the described system. The energy supply of Pantelleria, due to the great distance from the Sicilian coast, is based on fossil fuels. It is energetically independent from the national grid and relies on a diesel power plant. This work aims to evaluate the power-to-power system capabilities, exploiting renewable energy sources and energy storage to supply the residential load and the public mobility, promoting the energy transition. In particular, the analysis is focused on a hybrid storage system based on hydrogen.

First of all, a brief hydrogen role and energy storage reviews are given. In the first case, the different uses of hydrogen and its production technologies are described. In the second case, an overview of the existing energy storage and a literature review of hybrid storage systems are developed. Then, the residential and transportation load is evaluated, as well as the RES potential of the island, focusing on solar and wind power production. The data obtained are used in a techno-economic optimization, able to minimize the LCOE. The results obtained are used to assess if the power-to-power systems are economically advantageous in isolated areas. Finally, an environmental analysis is performed, in particular the avoided CO_2 emissions are evaluated.

CHAPTER 2

GENERAL FRAMEWORK OF ENERGY STORAGE

2.1 Hydrogen Role

Hydrogen represents a valuable option in the reduction of greenhouse gas emissions. It can be seen as a clean solution only if both the feedstock and the production are free of emissions (6). It is a multi-purpose carbon-neutral energy carrier, whose use can be subdivided into three categories:

- Hydrogen as end-use fuel
- Hydrogen as feedstock to produce carbon-neutral hydrocarbons
- Hydrogen as a carrier of chemical storage of electricity

Nevertheless, despite these potential uses, at present hydrogen is mainly exploited in industrial applications, in the petrochemicals industry and refineries. Moreover, hydrogen has faced different barriers, like costs and availability of infrastructure (13).

The hydrogen can be classified depending on the way it is produced (6):

- **GREY HYDROGEN:** the hydrogen is produced by steam methane reforming (SMR). The emissions are comparable with natural gas combustion.
- **BLUE HYDROGEN:** the hydrogen is always obtained from SMR, but it is associated with CCS to avoid emissions.
- **GREEN HYDROGEN:** the hydrogen comes from a carbon-free process, that uses electrolysis. The main driver, in this case, is the electricity that can be produced from RES.

2.1.1 Hydrogen as end-use fuel

Hydrogen can be used as a fuel, in this way it is possible to replace all the applications based on fossil fuels. In particular, hydrogen can improve the transport sector using fuel cells. This technology can be implemented in means of transport like buses or trains. In this framework, refueling stations are required and, economically, could be more convenient to produce and store the hydrogen on-site (6). Moreover, this would help in case of security issues, like leakage. As well as the transport sector, also the residential sector can benefit from hydrogen for heating and cooking purposes (14).

2.1.2 Hydrogen as feedstock to produce carbon-neutral hydrocarbons

Synthetic fuel, produced by the synthesis of hydrogen or through syngas and carbon dioxide, can substitute fossil fuels without changing the infrastructure and the equipment (6). The principal drawbacks are represented by the high cost compared to the traditional fossil fuels and the CO_2 emissions during the combustion, which is not consistent with the sustainable pathway started.

2.1.3 Hydrogen as a carrier of chemical storage of electricity

The decarbonized generation is feasible only if is fully based on RES. This requires the use of storage, in particular chemical storage based on hydrogen, to face the intermittency. This energy vector is interesting because it is relatively easy to be stored in large quantities and for the long term (15). The stored hydrogen can be converted into electricity with the use of a fuel cell.

2.2 Energy Storage

RES must be linked to energy storage because their intermittent availability represents the main issue for their penetration in the energy scenario. Energy storages bring with them advantages for the electrical system like load levelling and peak shaving, but also improving power quality and reliability (16). In literature, energy storage can be classified in four categories:

2.2.1 Stationary Battery Energy Storage

Batteries are a mature technology, that is characterised by high energy densities and high voltages (16). The main battery types are represented by lithium-ion batteries and redox flow batteries (17). The former is exploited in electronic devices and, increasingly, in electric mobility. The latter has a long service life because the degradation of electrodes and electrolytes is minimal. The following tables summarise the advantages and disadvantages of both batteries.

Advantages	Disadvantages
High specific energy No maintenance High capacity, low internal resistance, good coulombic efficiency Reasonably short charge times	Need for protection circuit to prevent thermal runaway when stressed Degradation at high temperature and when stored at high voltage Impossibility of rapid charge at low temperatures (<0°C) Need for transportation regulations when shipping in larger quantities

Table 1 Advantages and Disadvantages of Lithium-Ion Batteries (17)

Advantages	Disadvantages
Long service life: have a system endurance period of 20 years, with an unlimited number of charge and discharge cycles available without degradation Versatility: with the output and the capacity of a battery capable of being designed independently of each other, these batteries allow flexible design. High safety: are capable of operating under normal temperatures and are composed of non-combustible or flame-retardant materials.	Complexity: their systems require pumps, sensors, flow and power management, and secondary containment vessels. Low energy density: the energy densities are usually low compared with those of other types of batteries.

Table 2 Advantages and Disadvantages of Redox Flow Batteries (17)

2.2.2 Mechanical Energy Storage

Among the mechanical energy storage, the compressed air energy storage (CAES) and the pumped hydro energy storage (PHES) stand out (16). In CAES the excess of energy power is exploited to compress air in an underground cavern. When the energy is needed, the pressurized air is expanded in a turbine that drives a generator. The PHES uses low-cost electricity to pump water into an upper reservoir. The water, from the upper reservoir, is injected into turbines when electricity is requested. The following tables list the advantages and disadvantages of CAES and PHES.

Advantages	Disadvantages
Potential for small-scale, on-site energy storage solutions as well as larger grid-scale installations that can provide sizable energy reserves for use in load shifting.	Low storage density: very large volume storage sites required. These sites are geologically constrained.

Table 3 Advantages and Disadvantages of CAES (17)

Advantages	Disadvantages
Very low cost of storage Provide energy-balancing, stability, storage capacity, and ancillary grid services such as network frequency control and reserves High efficiency and benefit in terms of balancing load within the overall power system.	Difficult to build due to implications of large water-based infrastructure and of executing massive construction projects

Table 4 Advantages and Disadvantages of PHES (17)

2.2.3 Thermal Energy Storage

This type of energy storage takes advantage of a storage medium, able to store thermal energy. Koohi-Fayegh et al. in (16) categorized them into sensible heat storage, latent heat storage and thermochemical energy storage. The first one stores energy in a medium through a temperature change, like water or rock. The second one exploits the phase change of materials and are interesting due to the absence of temperature change of the process. The third one uses chemical reactions to store energy. This process is composed of three phases: endothermic dissociation, storage of reaction products and exothermic reaction of the stored products. The advantages are represented by the lower losses and higher energy densities than sensible/latent heat storage.

2.2.4 Chemical Energy Storage

Chemical energy storage exploits a reversible chemical reaction to store energy. The most interesting is the electrochemical energy storage, in which electrical energy that comes, for example, from RES can be used to drive the chemical reaction. The main representative of this category of storage is hydrogen energy storage, in which hydrogen is produced and stored, when a surplus of energy occurs, and then is exploited to produce electricity. In this framework, an electrolyser and a fuel cell, coupled with a hydrogen tank, are the most interesting devices, since this process can be completely carbon-free and can promote RES penetration.

CHAPTER 3

SITE DESCRIPTION

Pantelleria is an island located in the middle Strait of Sicily in the Mediterranean Sea. It is interesting from the energy point of view because it is the first in size among the non-interconnected minor island in Italy. Its total area is equal to 84,5 km^2, with 7665 inhabitants (18) that are permanently resident in the island. The previous number varies seasonally due to the tourism flows. Pantelleria can be subdivided in eleven districts: Pantelleria centro, Scauri, Khamma, Tracino, Rekhale, Sibà, Bukkuram, San Vito, Grazia, Campobello and Bugeber.

Fig. 8 Map of Pantelleria (19)

The energy supply of the island is expensive due to its location because it is not connected to the electric national grid. It relies on fossil fuels, where S.MED.E. Pantelleria S.p.A. owns the power plant, in which diesel is used. The plant is composed by 8 diesel generators, with a total of 23 MW (20). The fuel is imported from Sicily by ferries. This is not only expensive, but also extremely polluting.

Nevertheless, the island is characterized by a high availability of RES, especially solar and wind sources. The solar one represents the most promising among the RES because it can be exploited everywhere. In fact, PV panels can be installed on the building's roof, instead of using a specific area. The annual solar radiation in Pantelleria is equal to 1.69 MWh/m^2, with a seasonal variation (21). As regards the wind source, its location ensures a good windiness, which can be exploited using a vertical axis wind turbine.

Now, the energy mix of the island relies also on the mentioned RES. The RES installed capacity is equal to 750 kW, subdivided into 720 kW of PV, where the largest plant's size is 90 kW, and 32 kW of wind turbines (20).

The locations of the renewable power plant installed on the island are available on the website "ATLAIMPIANTI" (22), in which the main power plants in Italy are collected. **Fig. 9** and **Fig. 10** are shown the RES plants in Pantelleria.

Fig. 9 PV power plants (22)

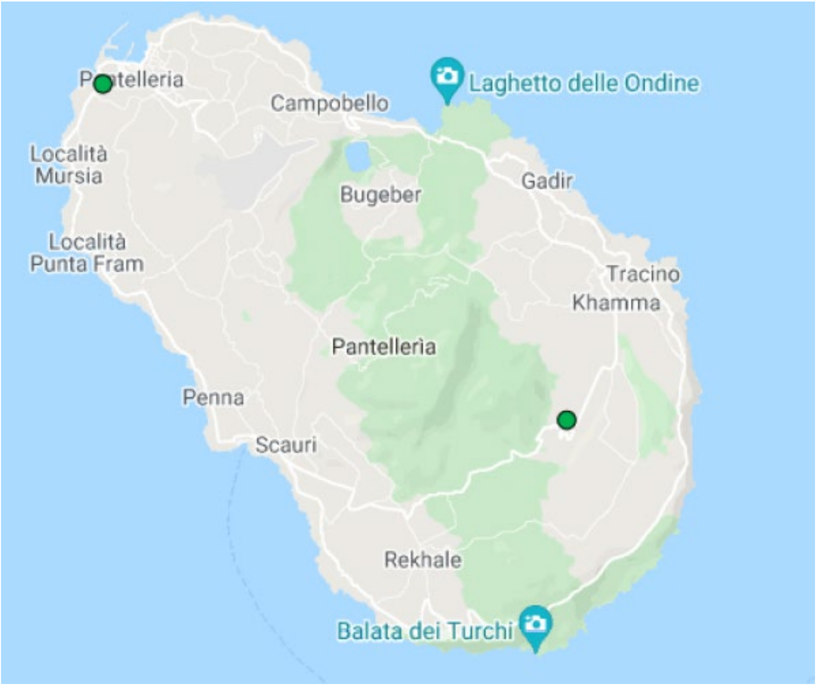

Fig. 10 Wind turbines (22)

Pantelleria, despite its current energetic configuration, potentially can be a fertile ground to explore a new layout consistent with the energy transition. Moreover, the results obtained from the study of a small area, can be used to rethink the energy strategies of larger areas. This general framework is useful to understand why Pantelleria can be a worthy candidate to estimate the potential of P2P systems.

CHAPTER 4

SYSTEM CONFIGURATION

In the new energy production layout of Pantelleria, the P2P system relies on solar PV panels and wind turbines. Solar and wind source have been chosen among other RES because the technology associated are sufficiently mature. The P2P plant studied aims to produce electricity to supply the residential load. In **Fig. 11** the entire system is outlined.

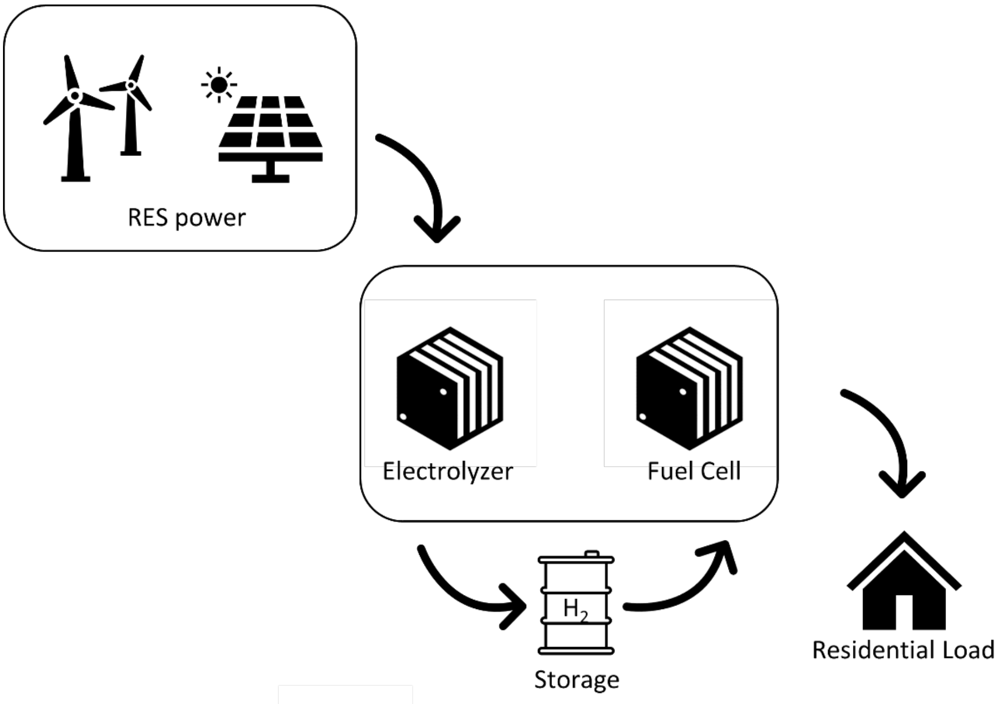

Fig. 11 P2P system layout

Also a P2G system is sized, that provide hydrogen to a refueling station, using only the solar power, and is able to feed a hydrogen bus fleet. In **Fig. 12** is shown the refueling station, while in the subsequent paragraphs, every single component is described.

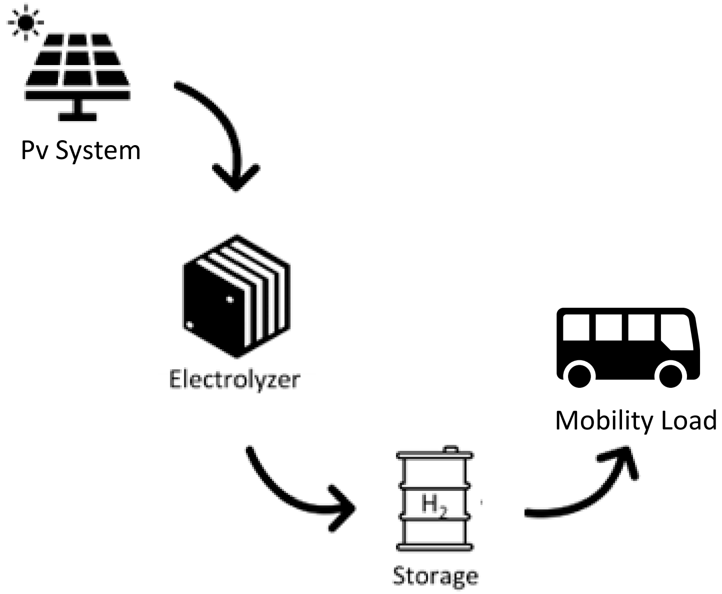

Fig. 12 P2G system layout

4.1 PV Power System

The photovoltaic power system is made of several modules connected together in order to obtain significant power. The base element of the module is represented by the solar cell. 36 or 72 cells connected in series generate a module. There are three types of modules: modules with monocrystalline silicon cells, modules with monocrystalline silicon cells and modules with thin-film amorphous silicon. Changing the PV module connection, the structure is named differently (23) (24):

- PV string: it is an independent production unit, in which a group of modules are connected in series.
- PV array: a support structure holds together a group of modules,
- PV field: a group of arrays is assembled forming a generator.

The photovoltaic system can be linked to the grid or work in a stand-alone mode. In this study, a stand-alone configuration is considered.

The power produced by this system can be obtained from the following equation (25):

$$P_{PV} = P_{\,PV,STC} f_{PV} \frac{G_T(t)}{G_{T,STC}} \left[1 + \alpha\left(T_c(t) - T_{c,STC}\right)\right]$$

Where $P_{PV,STC}$ is the rated PV power [kW], f_{PV} is the derating factor [%], G_T is the solar radiation incident on the PV array [kW/m^2], G_{STC} is the incident radiation at standard test conditions [1 kW/m^2], α is the temperature coefficient of power [%/°C], T_c is the PV cell temperature [°C] and $T_{c,STC}$ is the PV cell temperature at standard test conditions [25°C].

The total solar incident radiation can be calculated as follow (26):

$$G_T(t) \; = \; G_{b,n}(t) \cdot cos(\theta) + G_{d,h}(t) \cdot F_{c,s} \; + G_{t,h}(t) \cdot \rho_g \cdot F_{c,g}$$

Where $G_{b,n}$ is the direct normal irradiance [kW/m^2], $G_{d,h}$ is the diffusive irradiance on the horizontal surface [kW/m^2], $G_{t,h}$ is the total irradiance on the horizontal surface [kW/m^2], ρ_g is the albedo of ground, $F_{c,s}$ is the collector-sky view factor, $F_{c,g}$ is the collector-ground view factor and θ is the angle of incidence of the beam solar radiation on the tilted surface.

The angle θ can be evaluated as follow:

$$\cos\theta = \cos\beta\cos\theta_z + \sin\beta\sin\theta_z\cos(\gamma_s - \gamma)$$

Where β is the slope of the tilted PV surface [°], θ_z is the zenith angle [°], γ_s is the solar azimuth angle [°] and γ is the azimuth angle of the PV surface [°].

The angle θ_z is obtained from the following relation:

$$\cos\theta_z = \cos\phi\cos\delta\cos\omega + \sin\phi\sin\delta$$

Where ϕ is the latitude [°], δ is the declination [°] and ω is the hour angle [°].

The declination and the hour angle are defined as:

$$\delta = 23.45\sin(360\frac{284+n}{365})$$

$$\omega = 15(h - h_{culm})$$

Where n is the day of the year, h and h_{culm} are the standard time and the noon time respectively. The two view factors are calculated as follow:

$$F_{c,s} = \frac{1+\cos\beta}{2}$$

$$F_{c,g} = \frac{1 - \cos\beta}{2}$$

The temperature of the cell can be evaluated using (27):

$$T_c(t) = T_a(t) + \frac{G_T(t)}{800}(NOCT - 20)$$

Where T_a is the ambient temperature [°C] and NOCT is the nominal operating cell temperature [°C].

In order to evaluate the power output from the PV system, the LG Neon R solar module is chosen. The data, from the specification sheet, useful for the calculation, are summarized in the following table:

PV Technical Specification

P_{rated}	365 W
NOCT	44°C
η	21%

Table 5 PV Datasheet

4.2 Wind Power System

The wind power system is composed by a wind turbine that is a device able to extract the energy from the wind producing electricity. A group of wind turbines in the same location is called wind farm. There are two types of wind turbine (28):

- Wind turbine with horizontal axis: this wind turbine is the most diffused and exceeds the height of 60 m above the ground by a support tower. The key elements of this device are the blades. Usually, 2 or 3 blades are used.
- Wind turbine with vertical axis: this device is exploitable in sites where the wind direction varies considerably. In fact, this turbine does not need to be pointed in the wind direction to work.

The power produced by the turbine can be evaluated using the power curve provided by the manufacturer and the wind speed extracted from PVGIS. It must be taken into account that the power curve is obtained in standard conditions and the provided wind speed is measured at the height weather station, equal to 10 m. In the case of Pantelleria, the temperature doesn't affect the air density and consequently, the power produced. Only the height considered affects the result because usually, the hub height exceeds 10 m. Therefore, the wind speed is corrected using the power law profile (29) of the form:

$$\frac{U(h)}{U(h_r)} = (\frac{h}{h_r})^{\alpha}$$

Where U(h) is the wind speed at hub height [m/s], U(h_r) is the reference wind speed at 10 m [m/s], h is the hum height [m], h_r is the reference height equal to 10 m [m] and α is the power law exponent. The power law exponent depends on different conditions, in particular it is possible to summarize its value in three different cases:

- <u>CASE 1</u>
  α is equal to 1/7 (=0.14) when any detailed information is provided and a stable flow is considered.
- <u>CASE 2</u>
  α can be evaluated as a function of velocity and height with the Justus expression (30). The correlation is:
  $$\alpha = \frac{0.37 - 0.088\ln(U(h_r))}{1 - 0.088\ln(\frac{h_r}{10})}$$
- <u>CASE 3</u>
  α can be evaluated using the Counihan correlation (30), where the exponent is a function of the surface roughness z_0 in m. The expression is the following:
  $$\alpha = 0.096\log_{10}(z_0) + 0.016\,(\log_{10}(z_0))^2 + 0.24$$
  Where z0 assumes values between 0.001 m and 10 m depending on the surface considered. Its values can be easily found in the literature.

In this work, the second correlation is used. The power curve can be obtained after choosing the wind turbine model. In this case, a medium-sized turbine is selected considering the strategy adopted in (20). WES100 wind turbine is chosen and Barbosa de Alencar et al. (31) provided the procedure to obtain the specific power curve equation. The related technical specification and the power curve from the datasheet are shown in the following figures.

Life expectancy	> 20 years
Maintenance	Twice a year
Rated power	100 kW
Cut in wind speed	<3 m/sec. (6.7mph)
Cut out wind speed	25 m/sec. (56mph)
Nominal wind speed	13 m/sec. (28mph)
Survival wind speed	60 m/sec. (134mph)
Passive power regulation	Pitching (blade-angle adjustment)
Active power regulation	Fully variable back-to-back IGBT system
Noise emission at 8 m/s	45dB(a) at 100m
Operating temperatures	From -20°C up to +40°C

Fig. 13 WES100 technical specifications (32)

Wind speed (m/s)	Power kW
0	0,0
1	0,0
2	0,0
3	1,0
4	2,9
5	6,0
6	11,0
7	17,7
8	27,3
9	39,2
10	53,8
11	68,4
12	82,8
13	89,1
14	95,9
15	98,7
16	99,5
17	100,0
18	100,0
19	100,0
20	100,0
21	100,0
22	100,0
23	100,0
24	100,0

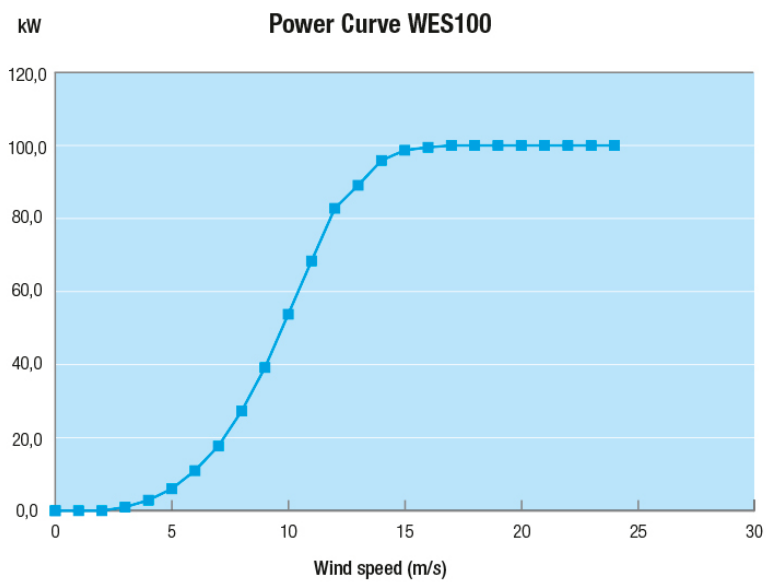

Fig. 14 WES100 power curve (32)

4.3 Electrolyzer

The electrolyzer is a device able to exploit the power to produce chemicals. In energy terms, the electrical energy is converted into chemical energy, therefore the Gibbs free energy difference is higher than zero. Electrolyzers take advantage of a chemical reaction, in particular a red-ox reaction. Usually, the main application of this machine is water electrolysis, in which H_2 and O_2 are extracted.

The structure of the electrolyzer is made of three layers: two electrodes and one electrolyte. The latter is placed among the two electrodes. The water electrolysis can be performed using two different electrolyzers, which differ for the material of the electrolyte:

- Alkaline electrolyzer: the electrolyte is liquid, composed of water and alkaline material (KOH or NaOH). It works at low temperatures, due to the liquid electrolyte.
- PEM (Polymeric Electrolyte Membrane) electrolyzer: the electrolyte is made of nafion. Compared to the previous electrolyte, nafion has higher conductivity.

Fig. 14 represents the schematic illustrations of the two electrolyzers.

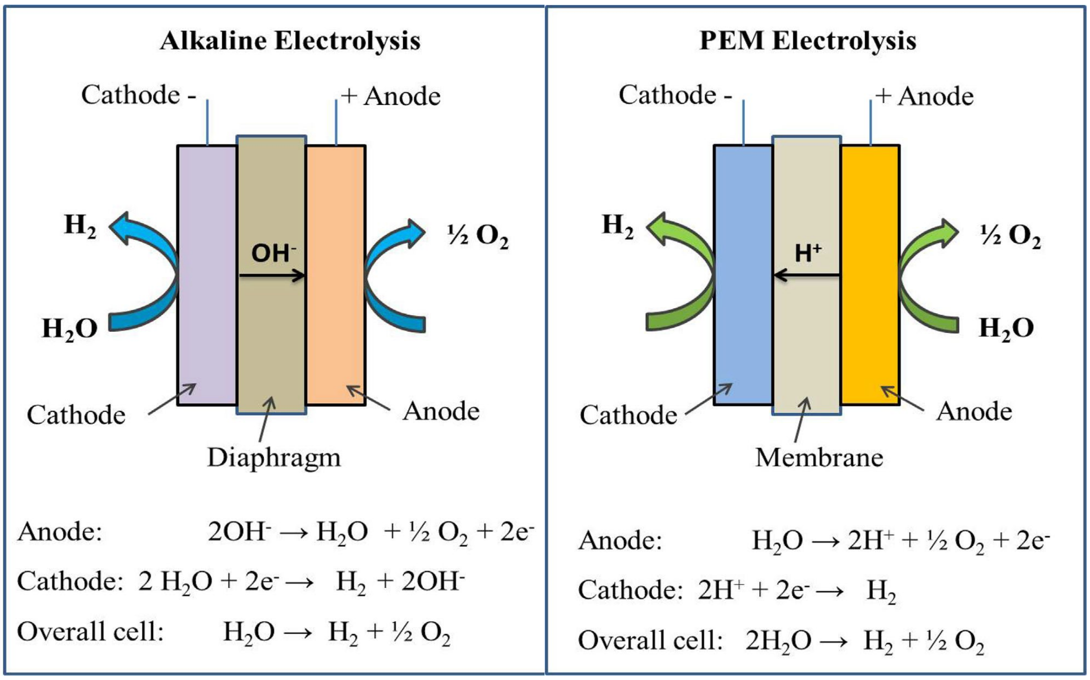

Fig. 15 Electrolyzers schematic illustration (33)

The operating electrolyzer voltage can be evaluated as follow:

$$V_c = E + V_{act} + V_{ohm} + V_{diff}$$

Where E is the Nernst voltage, V_{act}, V_{ohm} and V_{diff} are the activation, ohmic and diffusion overvoltages, respectively.

The expression of the Nernst equation is:

$$E = \frac{\Delta g_{reaction}(T, p_0)}{z_{fuel}F} + \frac{RT}{z_{fuel}F} \ln \left(\frac{\prod(\frac{p_i}{p_0})^{v_{i,P}}}{\prod\left(\frac{p_i}{p_0}\right)^{v_{i,R}}}\right)$$

4.4 Fuel Cell

The fuel cell is an electrochemical cell that works in a reverse way compared to the electrolyzer. In energy terms, the chemical energy is converted into electrical energy, therefore the Gibbs free energy difference is lower than zero.

In this study a PEM (Proton Exchange Membrane or Polymeric Electrolyte Membrane) fuel cell is adopted, where H_2 and O_2 are used to produce electricity. A group of fuel cells is called stack. This fuel cell has a structure slightly different from the electrolyzer one. The layers are:

- Catalyst layer: it is the active layer that allows the charge and ion transfer.
- Diffusion layer: it is a layer that supports the previous one. It must have good porosity and good conductivity for electrons.
- Gasket: it is a layer that avoids leakages. The material used can be nafion.
- Interconnector: it is a layer able to conduct electrons in the next cell. Usually, dense graphite is used.
- Electrolyte: it is a layer that conducts ions. It should be as thin as possible to reduce the ohmic drop. If it is too thin, electronic conduction occurs, bringing the system to the short circuit. Therefore, the thickness depends on the material used. The most used polymeric material is nafion, obtained from Teflon to which hydrogen sulphite is added.

Fig. 15 represents the PEM fuel cell reactions and structure.

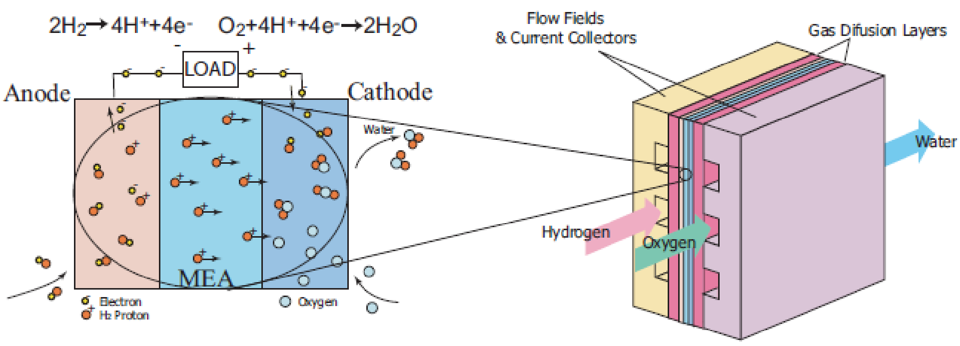

Fig. 16 PEMFC reactions and structure (34)

The operating fuel cell voltage can be evaluated as follow:

$$V_c = E - V_{act} - V_{ohm} - V_{diff}$$

Where E is the Nernst equation, V_{act}, V_{ohm} and V_{diff} are the activation, ohmic and diffusion overvoltages, respectively.

The expression of the Nernst equation is:

$$E = -\frac{\Delta g_{reaction}(T, p_0)}{z_{fuel}F} + \frac{RT}{z_{fuel}F}\ln\left(\frac{\prod(\frac{p_i}{p_0})^{v_{i,R}}}{\prod\left(\frac{p_i}{p_0}\right)^{v_{i,P}}}\right)$$

4.5 Hydrogen Refueling Station

The bus fleet studied is designed to promote the energy transition, therefore fuel cell electric vehicles are chosen. The fuel exploited, according to the system configuration, is hydrogen, so a refueling station must be planned. According to Qin et al. (35), the common hardware of the refueling station includes a hydrogen production equipment, a purification system, a storage vessel, a compressor, a safety, mechanical and electrical equipment.

In this paper, the refueling station is designed to produce hydrogen on-site using water electrolysis. The configuration includes the following components (36):

- Electrolyzers: the hydrogen obtained from water electrolysis has a high value of purity and it is relatively simple to produce it.
- Compressors: the hydrogen must be pressurized before being injected into the vehicle. Therefore, a compressor is essential.

- Hydrogen storage tanks: the hydrogen produced by electrolysis is higher than the demand, so a storage is added to the station configuration.
- Cooling system and dispensers: the hydrogen must be cooled down before the refueling of the vehicle because is subjected to an increase in temperature.

The electrolyzer and the hydrogen storage are also used to supply the residential load, so the compressor is placed after the hydrogen tank to save energy. There are two standard pressure levels in the transport sector: 350 bar and 700 bar (37). In general, light-duty vehicles, like cars, use the higher pressure level for the hydrogen tanks to maximise the mass of hydrogen stored per unit volume. While heavy-duty vehicles, like buses, use the lower pressure level. Considering a bus fleet, with a pressure of 350 bar, is an advantage from the economic point of view.

CHAPTER 5

DATA ESTIMATION

The input data useful to carry out the study are the residential load, the mobility load and the meteorological variables needed to evaluate the solar and wind potential.

5.1 Residential Load

The highest amount of end-use electricity is attributable to the residential sector (20). Therefore, the residential electrical load must be satisfied by the system. As an input vector, the annual hourly load is required, but on-site measurements are not available, so it is necessary to rely on literature data. The annual load demand is extracted from (38), in which the hourly profile of Ginostra village, on the island of Stromboli (Southern Italy), is given.

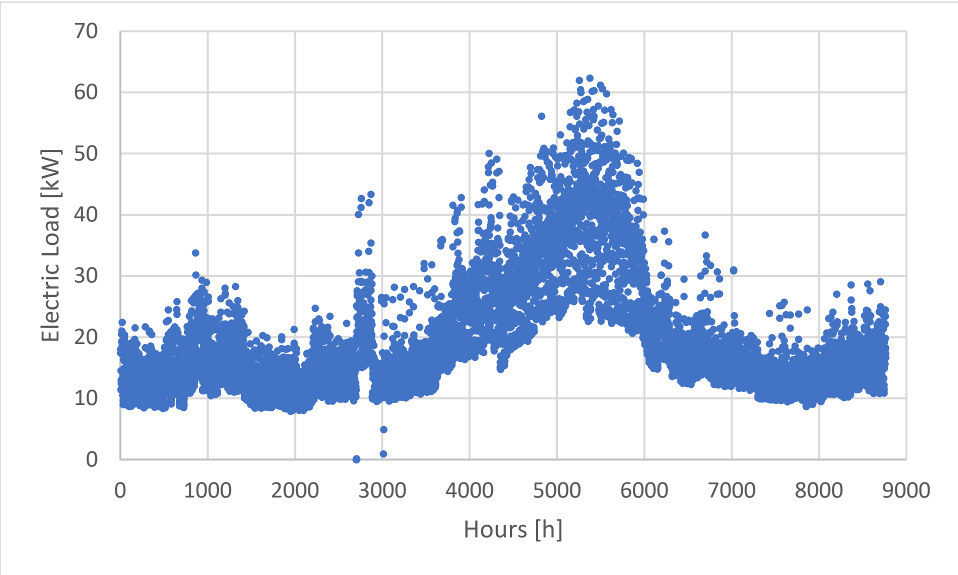

Fig. 17 Hourly electricity consumption of Ginostra in 2015 (38)

It can be used as a reference profile because the highest electrical demand of Ginostra comes from the residential sector and varies seasonally, due to tourism flows, as it happens in Pantelleria. In literature, only the annual residential load of Pantelleria in 2018 is provided and it was equal to 11719 MWh (20). These two elements are exploited to extract the hourly electrical load of Pantelleria. Specifically, the previous hourly consumption is scaled with the total yearly load of Ginostra, the result obtained that is multiplied by the total yearly load of Pantelleria.

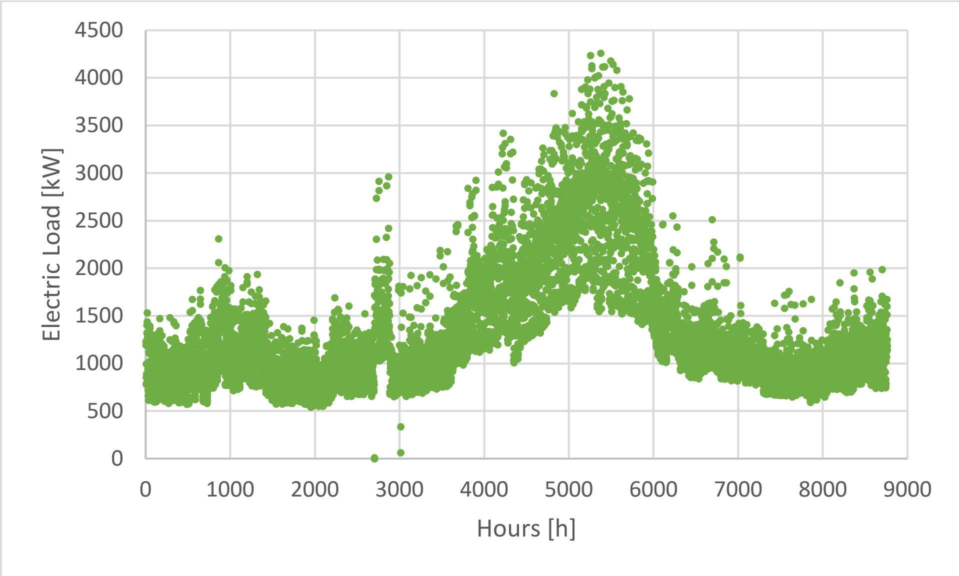

Fig. 18 Hourly electricity consumption of Pantelleria

In this way, the shape of the load profile remains unchanged, while the annual load is met. The monthly electricity consumption is shown in **Fig. 18**.

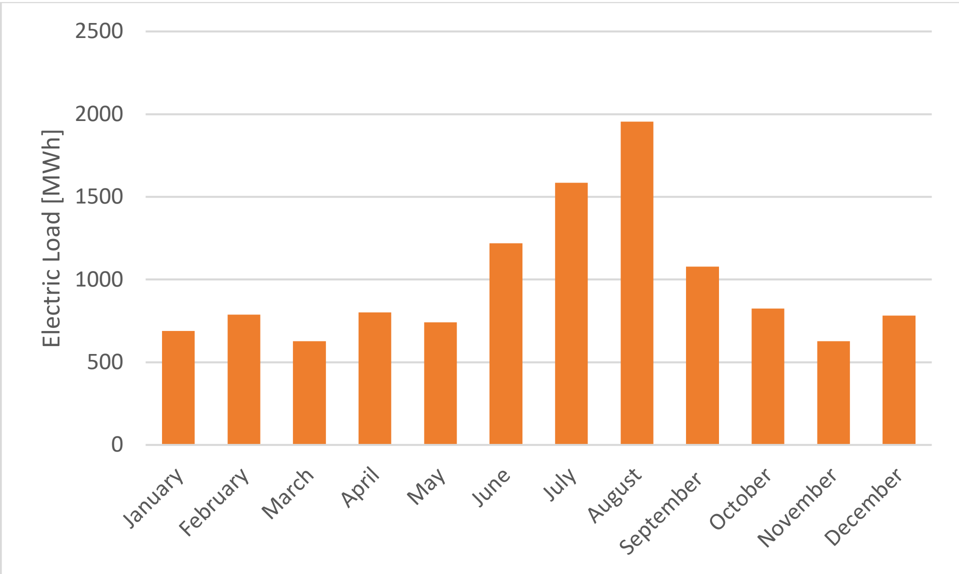

Fig. 19 Monthly electricity consumption

In *“Clean Energy Transition Agenda: Pantelleria”* (20), the monthly electricity load is given. **Fig. 19** includes the overall electricity consumption. The residential electricity demand is equal to the 40% of the total load, then the previous profile load can be considered a good approximation.

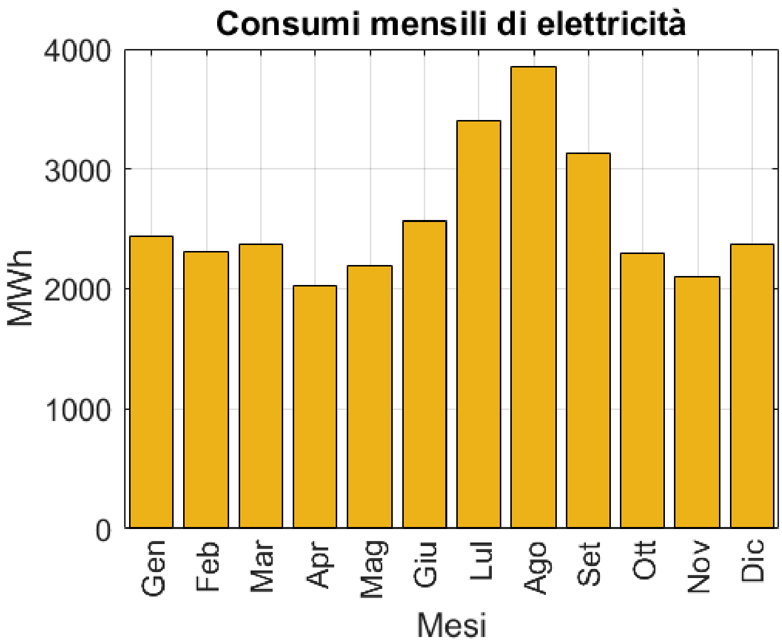

Fig. 20 Measured monthly electricity consumption (20)

5.2 Mobility Load

The public transport of Pantelleria consists of a bus fleet with 7 components. In the new system configuration, it is necessary to estimate the amount of hydrogen useful to make fuel cell buses work. The routes covered by the public transport are shown in **Table 6**.

	NUMBER OF RACES		
	Path Length [km]	Winter	Summer
Pantelleria – Tracino	13	7	7
Tracino - Pantelleria	13	7	7
Pantelleria – Aeroporto – Buccuram – Sibà	34,5	4	4
Sibà – Buccuram – Aeroporto – Pantelleria	34,5	4	4
Pantelleria – Aeroporto	6,5	3	5
Aeroporto – Pantelleria	6,5	3	5
Pantelleria - Rekale	16	7	7
Rekale - Pantelleria	16	7	7
Pantelleria – Bugeber	10	2	2
Bugeber – Pantelleria	10	2	2

Table 6 Routes covered by the public transport (20)

The heavily populated areas of Pantelleria are Pantelleria Centro, Khamma-Tracino and Scauri. Therefore, in this study, only the routes that link the aforementioned areas are considered (Pantelleria – Tracino - Pantelleria, Pantelleria - Rekale - Pantelleria).

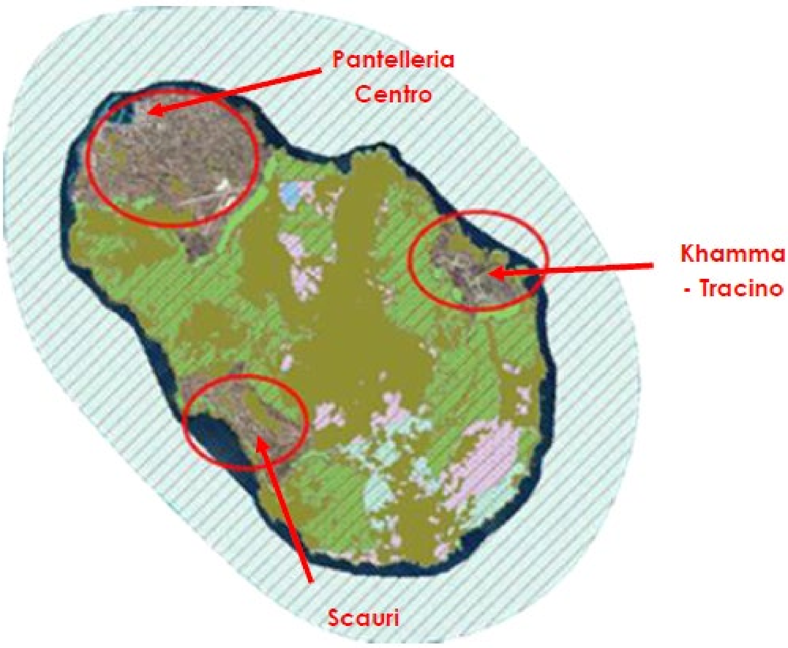

Fig. 21 Heavily populated areas of Pantelleria (20)

Considering that the summer season lasts 92 days, while the winter season last the remaining 273 days, it is possible to estimate the kilometres travelled in a year. The results obtained are summarized in **Table 7**.

	km/day	km/year
Pantelleria – Tracino – Pantelleria	182	66430
Pantelleria – Rekale – Pantelleria	224	81760

Table 7 kilometres covered by the bus fleet

According to (39) the amount of gasoline consumption has been set equal to 0.4 l/km, while the hydrogen consumption has been set equal to 0.09 kg/km. In this way, it is possible to evaluate the hydrogen needed for the sizing of the system. The gasoline and hydrogen consumptions are shown in **Table 8**.

	Gasoline [l/day]	Hydrogen [kg/day]	Gasoline [l/year]	Hydrogen [kg/year]
Pantelleria – Tracino – Pantelleria	72.8	16.38	26572	5978.7
Pantelleria – Rekale – Pantelleria	89.6	20.16	32704	7358.4

Table 8 Gasoline and hydrogen consumption

5.3 Solar Potential

According to the *"Clean Energy Transition Agenda: Pantelleria"* (20), the most suitable area for PV production is the Arenella area. The input data useful to evaluate the power output from the solar source are ambient temperature and the global irradiance on the PV surface. These variables can be extracted from PVGIS (40) which is a tool useful to obtain meteorological data. In this study, the Typical Meteorological Year (TMY) is adopted. The TMY is a data set containing the average weather conditions over a time period (41), in this case, 10 years or more. Usually, the dataset includes the hourly value of solar radiation, ambient temperature, humidity, wind speed and wind direction. The ambient temperature and the solar irradiance profiles are shown in Fig. 21 and **Fig. 22**, respectively.

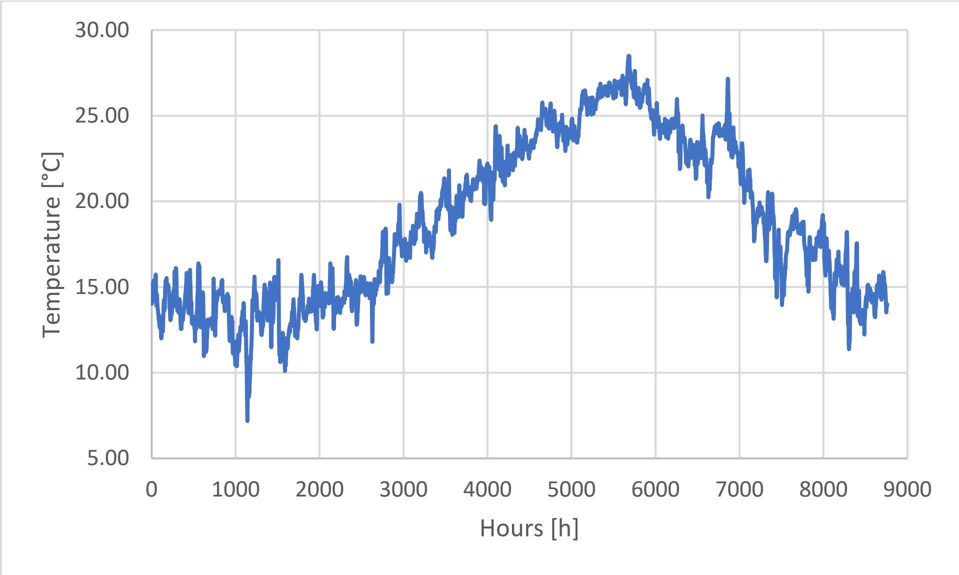

Fig. 22 Ambient temperature profile

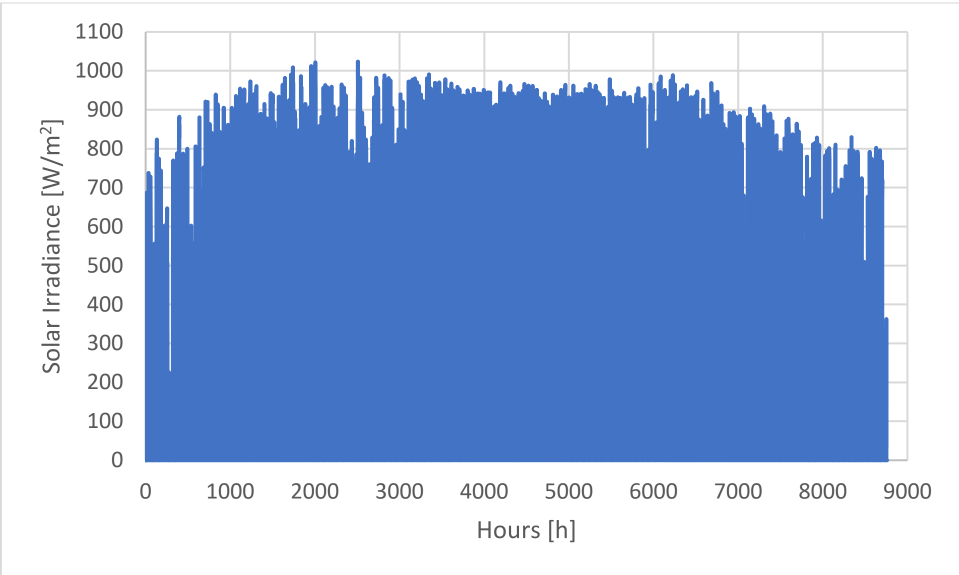

Fig. 23 Global irradiance on a PV surface

According to Section 4.1, the PV power production is evaluated considering the optimal value for β and γ, 34° and 4° respectively.

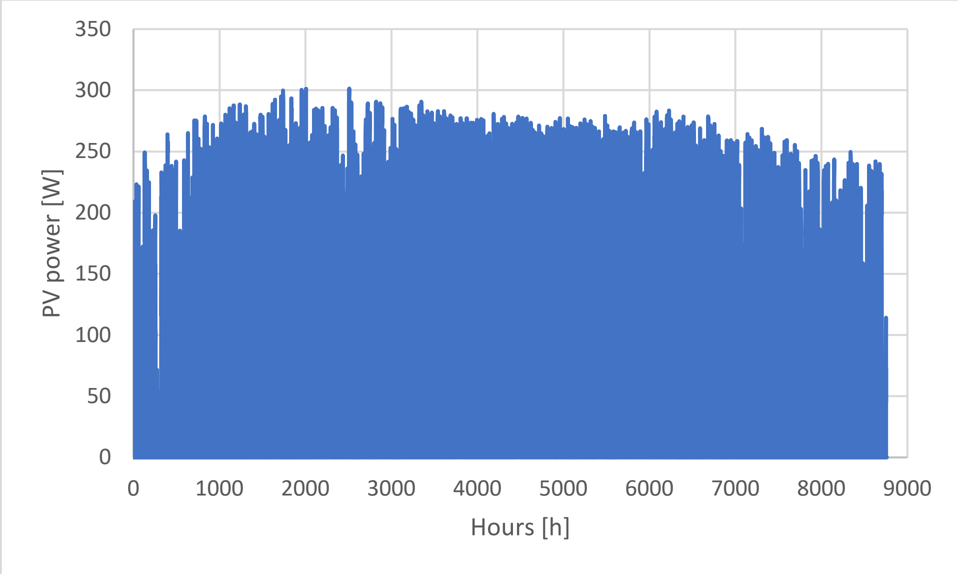

Fig. 24 PV power output

5.4 Wind Potential

The wind power production evaluation needs a data set that can be extracted from PVGIS using the previous procedure, in which a TMY is considered. The wind speed at a reference heigh is needed, in this study 10 m is the height considered. The wind speed throughout the year is shown in **Fig. 24**.

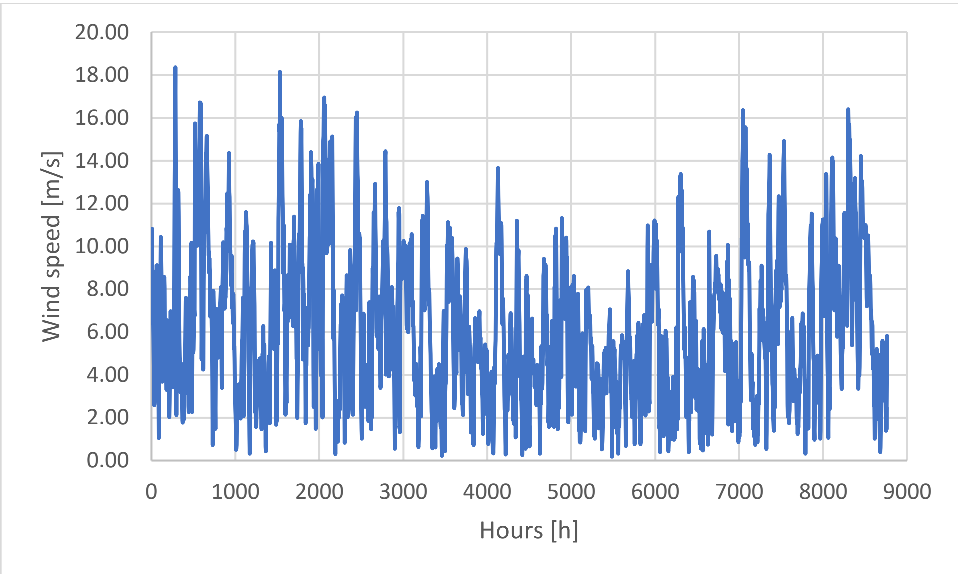

Fig. 25 Wind speed at 10 m height

Using a simple MATLAB code and following the procedure described in Section 4.2, the wind power production is obtained.

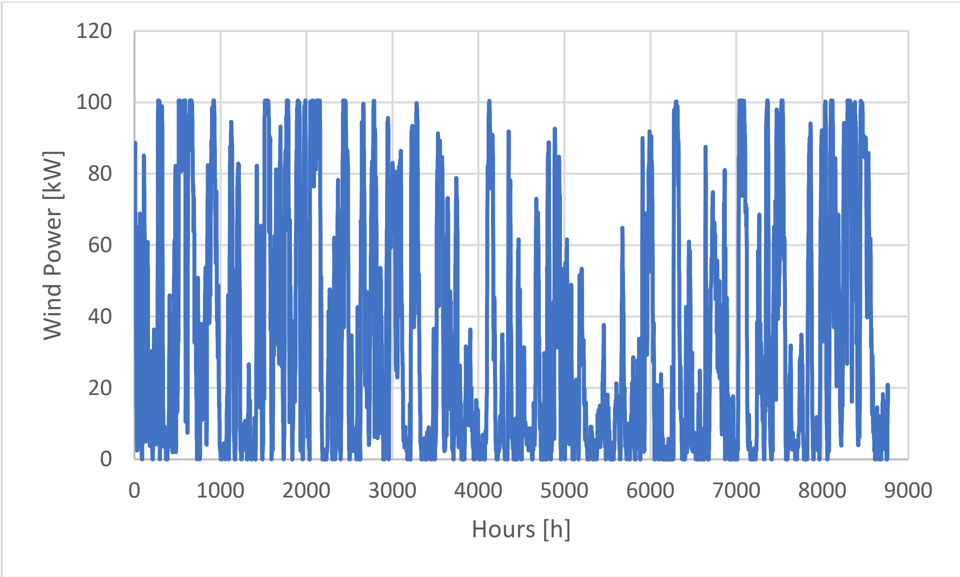

Fig. 26 Wind power output

CHAPTER 6

SIZING METHOD AND SYSTEM OPTIMIZATION

6.1 Particle Swarm Optimization

The particle swarm optimization (PSO) is a meta-heuristic optimization technique (42), able to simulate animal social behaviour. A set of particles, called swarm, defined by a position and a velocity vectors (43), move towards their best solution after a certain number of iterations. The iteration process does not require a good initial solution. The global best solution is obtained through different steps:

- STEP 1: the optimization technique starts setting the parameters for the iterations summed in the following table.

Parameter	**Value**
Population Size	300
Minimum adaptive neighborhood size	0.75
Cognitive learning coefficient	1.9
Social learning coefficient	1.9

Table 9 Parameters of the PSO

- STEP 2: the starting velocities and the positions of each particle are defined, setting random values.
- STEP 3: the positions and the velocities of particles is updated using the following equations:

$$X_i^{k+1} = X_i^k + v_i^{k+1}$$

$$v_i^{k+1} = [\omega v_k^i + C_1 r_1 (P_i^k - X_i^k) + C_2 r_2 (P_g^k - X_i^k)]$$

Where v_k^i and v_i^{k+1} represent the velocities, $C_1 r_1 (P_i^k - X_i^k)$ is the cognitive component and $C_2 r_2 (P_g^k - X_i^k)$ is the social component.

- STEP 4: after a certain number of iterations, the final best solution is obtained.

In this work, the optimal size of each component is obtained using the described technique, while the Levelized Cost of Energy (LCOE) is minimized. In particular, the minimization process is limited by the following constraints:

$$S_{i,min} \leq S_i \leq S_{i,max}$$

$$LPSP \ \leq LPSP_{target}$$

Where S_i represents the size of the i-th component, LPSP is the Loss of Power Supply Probability, defined as the ratio between the annual energy that the system fails to meet and the annual required demand:

$$LPSP = \frac{\sum_{t=1}^{T} P_{DEFICIT}(t) \cdot \Delta t}{\sum_{t=1}^{T} P_{LOAD}(t) \cdot \Delta t}$$

6.2 Energy Management Strategy

The P2P system must be able to cover the load demand and protect every single component. Therefore, an energy management strategy (EMS) is useful to investigate if the system works properly. In this work, the EMS of the European REMOTE project is used, when only the residential load is considered. It can be summed up in two strategies (44):

- CASE 1: the storage solution is represented only by the hydrogen tank.
- CASE 2: the storage solution is represented by a battery (short-term storage) and the hydrogen tank (long-term storage).

The second strategy is more efficient because the number of start-ups of the fuel cell and the electrolyzer are limited (45). Moreover, the battery does not work over its operating limits, avoiding its degradation and a loss of performance.

In both cases, a simulation using MATLAB is carried out, in which at each time step the battery state of charge (SOC) and the storage level of hydrogen (LOH) are evaluated (46). The SOC is defined as follow:

$$SOC(t+1) = SOC(t) + \frac{P_{BT,c}(t)\ \Delta t\ \eta_{BT,c}}{C_{BT}} - \frac{P_{BT,d}\Delta t}{\eta_{BT,d} C_{BT}}$$

Where $P_{BT,c}$ and $P_{BT,d}$ are the charging and discharging power of the battery, $\eta_{BT,c}$ and $\eta_{BT,d}$ are the charging and discharging battery efficiencies and C_{BT} represents the nominal capacity of the battery. While the LOH is defined as follow:

$$LOH(t) = LOH(t-1) + \frac{P_{EL}(t-1)\,\Delta t\,\eta_{EL}}{C_{H_2}} - \frac{P_{FC}(t-1)\Delta t}{\eta_{FC} C_{H_2}}$$

Where P_{EL} and P_{FC} are the electrolyzer and fuels powers, η_{EL} and η_{FC} are the electrolyzer and fuel cell efficiencies and C_{H_2} represents the capacity of the hydrogen storage tank.

In the simulation code, the following values are used:

Parameter	Value
Minimum battery SOC	0.2
Maximum battery SOC	1
Minimum storage LOH	$\frac{p_{min}}{p_{max}} = \frac{3}{28}$
Maximum storage LOH	1

Table 10 SOC and LOH values

A third EMS is considered, in which only the refueling station (PV-electrolyzer-hydrogen storage) is involved. Therefore, hydrogen is used as the only source of energy for the system and only the mobility load is covered. In this configuration, the hydrogen demand is used to size the PV system, the electrolyzer and the hydrogen storage. This system is sized without optimization.

6.2.1 Only Hydrogen Configuration (Residential Load)

In this configuration, only the residential load is considered and both discharging and charging cases are evaluated. In the first situation, the load is higher than the power produced by the RES. Therefore, the remaining load is covered by the fuel cell. If the power given by the fuel cell is not enough, an external source is used.

In the second situation, the load is lower than the power produced by the RES. Therefore, the entire load is covered by the RES, and the power surplus is stored, as hydrogen, in a tank, with the help of the electrolyzer. If the power produced by RES exceed, the remaining part is exceeded. In both cases, the batteries, the fuel cell and the electrolyzer intervene when they do not exceed the minimum and the maximum values of the SOC and LOH.

Fig. 26 and **Fig. 27** show the logical block diagrams for both cases.

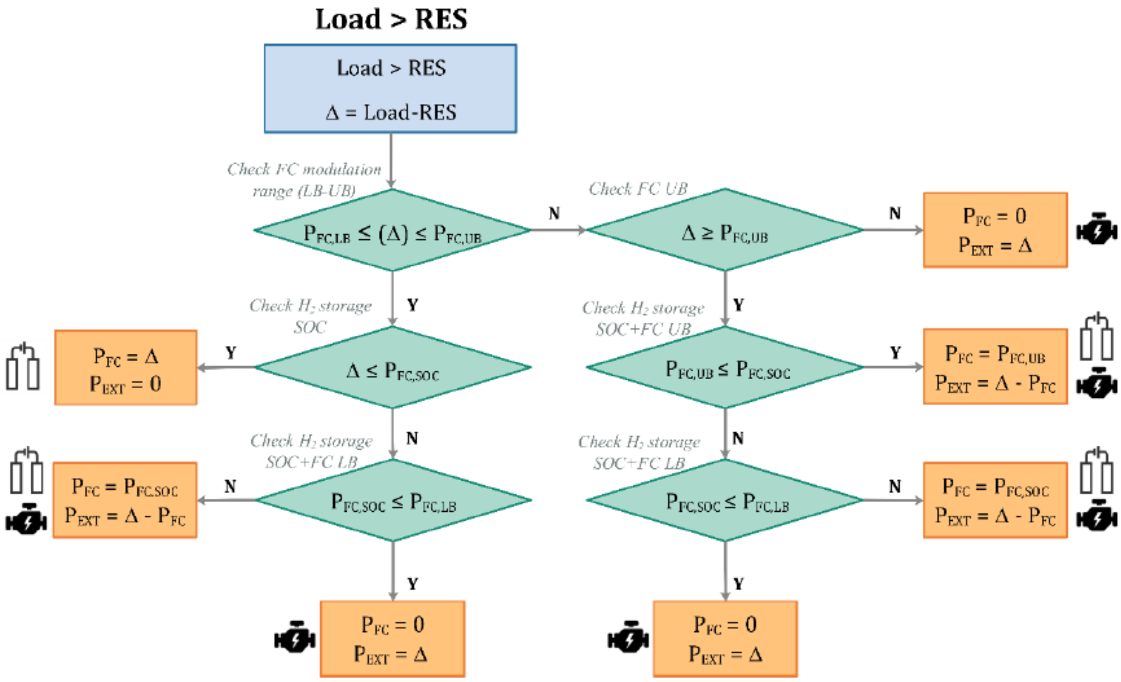

Fig. 27 Logical block diagram for the discharging case (44)

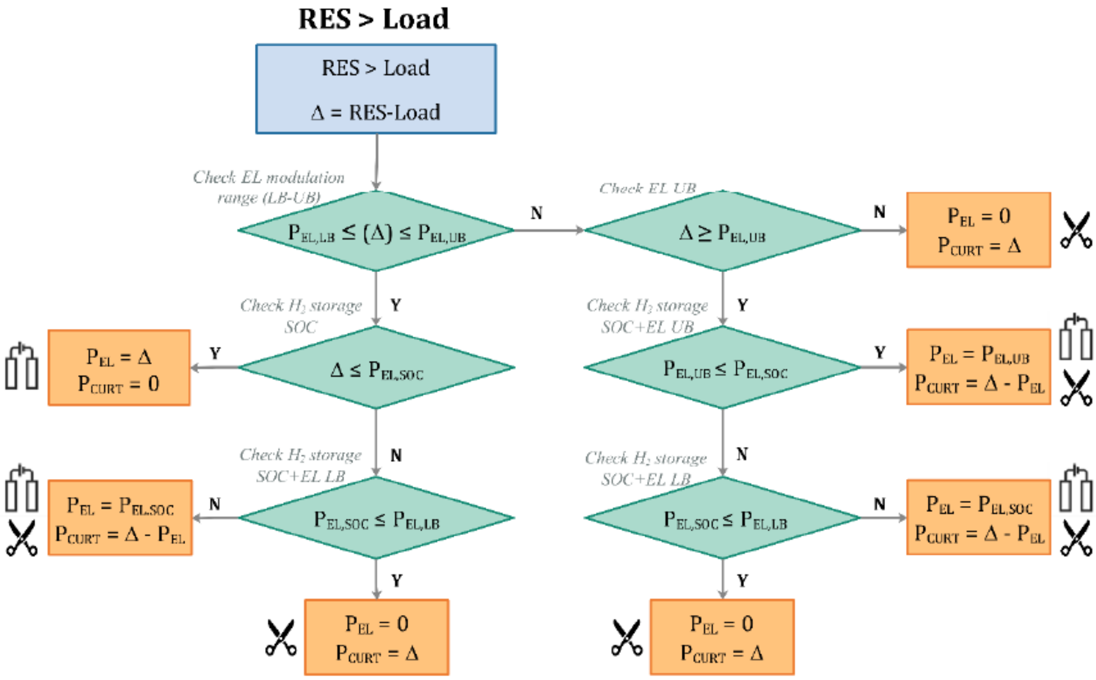

Fig. 28 Logical block diagram for the charging case (44)

6.2.2 Hydrogen and Battery Configuration (Residential Load)

Even in this scenario, two cases are analysed and only the residential load is considered. In the first one, the power produced by RES is lower than the demand. The unsatisfied load, if it is not too high, is covered by the battery, otherwise the fuel cell or an external source intervene.

On the contrary, when the RES power output exceeds the load, firstly the battery is charged and then, if the SOC maximum value of the battery is exceeded, the electrolyzer is used, to store hydrogen in the tank, or curtailed.

Fig. 28 and **Fig. 29** show the logical block diagrams for both cases.

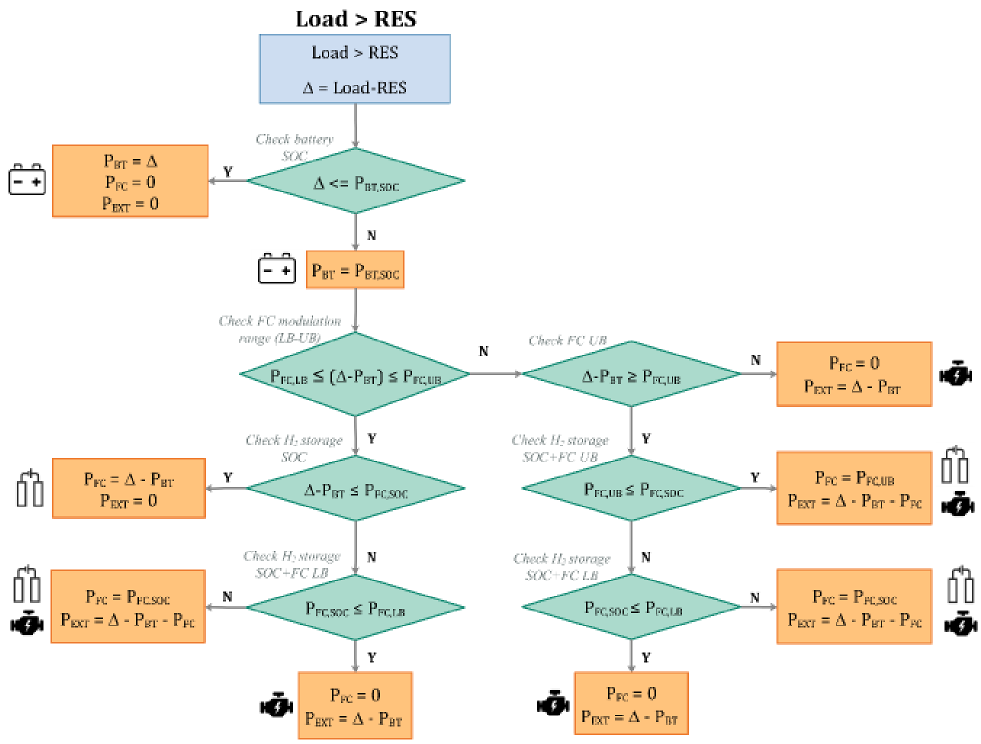

Fig. 29 Logical block diagram for the dicharging case (44)

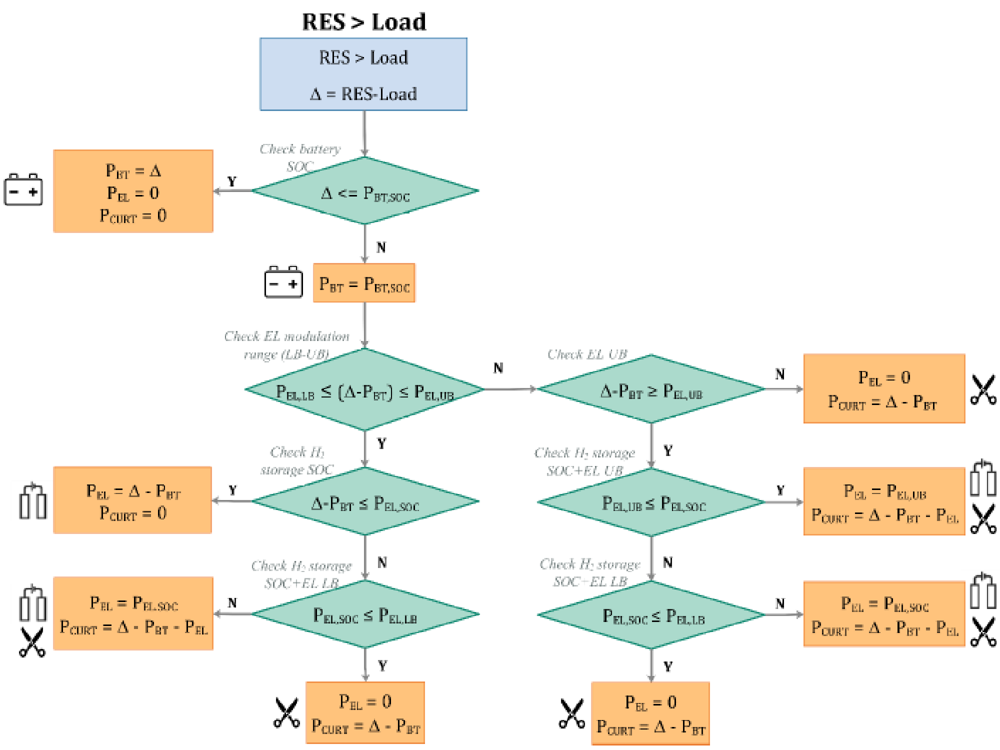

Fig. 30 Logical block diagram for the charging case (44)

CHAPTER 7

ECONOMIC ANALYSIS

7.1 CAPEX, OPEX and Replacement Cost

The economic analysis can be carried out after the evaluation of the capital expenditure (CAPEX), the operating expenditure (OPEX) and the replacement cost of every single component of the system.

The CAPEX represents the total investment cost and it is defined as follow:

$$CAPEX_{component} = CAPEX_{unit}S_{component}$$

Where $CAPEX_{unit}$ is the unitary CAPEX of the component and $S_{component}$ is the size of the component. The CAPEX of the system must be evaluated as the sum of the CAPEX of each component.

The OPEX considers all the running and maintenance costs, which are distributed throughout the project lifetime. Usually is defined as a unitary per year cost or as a percentage of the unitary CAPEX. It is evaluated using the following relation:

$$OPEX_{component} = OPEX_{unit}S_{component}t_{project}$$

Where $OPEX_{unit}$ is the unitary OPEX of the component, $S_{component}$ is the size of the component and $t_{project}$ is the lifetime of the system. The OPEX of the system must be evaluated as the sum of the OPEX of each component.

The replacement cost (RC) is the recurrent cost that must be sustained to replace the considered component during its entire lifetime.

The total cost of the system can be calculated as the sum of the total CAPEX, OPEX and replacement cost:

$$Total\ Cost = CAPEX + OPEX + RC$$

7.2 NPC

The Net Present Cost (NPC) of a system is the present value of the CAPEX, OPEX and replacement cost over the entire lifetime of the plant. This parameter can be evaluated as follow:

$$NPC = \sum_{i=1}^{comp} CAPEX_i + \sum_{n=1}^{lifetime} \frac{\sum_{i=1}^{comp} OPEX_i}{(1+d)^n} + \sum_{n=1}^{lifetime} \frac{\sum_{i=1}^{comp} RC_i}{(1+d)^n}$$

Where n represents the year considered and d represent is the real discount rate. The latter can be evaluated as follow:

$$d = \frac{d' - ir}{1 + ir}$$

Where d' is the nominal discount rate and ir is the inflation rate. Assuming that $d' = 7\%$ and $ir = 2\%$, the real discount rate is equal to 4.9%.

7.3 LCOE and LCOH

The Levelized Cost of Energy (LCOE) and the Levelized Cost of Hydrogen (LCOH) are two indexes defined as the minimum energy/hydrogen selling price, expressed in €/MWh and €/kg respectively, required to break even. The lifetime of the plant and the costs incurred in the construction, operation and maintenance are taken into account. They are defined as:

$$LCOE = \frac{\sum_{i=1}^{comp} CAPEX_i + \sum_{n=1}^{lifetime} \frac{\sum_{i=1}^{comp} OPEX_i}{(1+d)^n} + \sum_{n=1}^{lifetime} \frac{\sum_{i=1}^{comp} RC_i}{(1+d)^n}}{\sum_{n=1}^{lifetime} \frac{Energy_j}{(1+d)^n}}$$

$$LCOH = \frac{\sum_{i=1}^{comp} CAPEX_i + \sum_{n=1}^{lifetime} \frac{\sum_{i=1}^{comp} OPEX_i}{(1+d)^n} + \sum_{n=1}^{lifetime} \frac{\sum_{i=1}^{comp} RC_i}{(1+d)^n}}{\sum_{n=1}^{lifetime} \frac{Energy_j}{(1+d)^n}}$$

7.4 Component costs

The economic analysis can be completed using the CAPEX, OPEX and RC of the components. These values are obtained from the literature or from the producer.

7.3.1 PV Power System and Inverter

The costs of the PV system are obtained from (45), in which the LG Neon R solar module is considered. In addition, the inverter must be considered, to transform the produced current, from direct to alternating. Their parameters are summed up in the following tables.

PV Power System

CAPEX	1133.33 €/kW
OPEX	24 €/kW/y
RC	680 €/kW
Transport and Installation	320 €/kW
Transport and Installation (RC)	360 €/kW
Lifetime	25 y

Table 11 PV power system economic parameters

Inverter

CAPEX	93.33 €/kW
OPEX	4 €/kW/y
RC	80 €/kW
Lifetime	10 y

Table 12 Inverter economic parameters

7.3.2 Wind Power System

The economic parameters related to the wind turbine are listed in the following table.

Wind Power System

CAPEX	1175 €/kW
OPEX	3% CAPEX
RC	723 €/kW
Lifetime	25 y

Table 13 Wind power system economic parameters

7.3.3 Fuel Cell

The costs of the fuel cell are obtained from (26), in which the investment cost evaluated using the following equation:

$$CAPEX_{FC} = c_{ref}\left(\frac{S_{ref}}{S_{comp}}\right)\left(\frac{S_{comp}}{S_{ref}}\right)^{n}$$

Where c_{ref} represents the reference specific investment cost, S_{ref} and S_{comp} are the reference size and the size of the fuel cell and n is the cost exponent of the power function. These parameters and the other costs are summed in the following table.

Fuel Cell

c_{ref}	3947 €/kW
S_{ref}	10 kW
n	0.7
OPEX	4% CAPEX
RC	26.7% CAPEX
Lifetime	5 y

Table 14 Fuel cell economic parameters

7.3.4 Electrolyzer

The parameters of the electrolyzer are extracted from (26), and also in this case the CAPEX is obtained with the same equation of the fuel cell:

$$CAPEX_{EL} = c_{ref}\left(\frac{S_{ref}}{S_{comp}}\right)\left(\frac{S_{comp}}{S_{ref}}\right)^{n}$$

Electrolyzer

c_{ref}	4600 €/kW
S_{ref}	50 kW
n	0.65
OPEX	4% CAPEX
RC	26.7% CAPEX
Lifetime	5 y

Table 15 Electrolyzer economic parameters

7.3.4 Hydrogen Storage

The economic data of the hydrogen storage are obtained from the REMOTE project. A pressure of 30 bar is considered, because only the hydrogen for the mobility is pressurized at 350 bar with a compressor.

Hydrogen Storage

CAPEX	470 €/kg
OPEX	2% CAPEX
RC	470 €/kg
Lifetime	35 y

Table 16 Hydrogen storage economic parameters

7.3.5 Battery

The battery is used in the configuration that considers only the residential load. Therefore, its economic values must be used.

Battery

CAPEX	550 €/kWh
OPEX	10 €/kWh/y
RC	550 €/kWh
Lifetime	10 y

Table 17 Battery economic parameters

7.4 Economic Analysis Results

7.4.1 Residential Load – Hydrogen

CASE 1: LPSP=0

The optimized configuration with a LSPS=0, in which the system is able to satisfy the load in every moment, is summarized in the following table.

Residential Load - Hydrogen

PV Power System	9282 kW
Wind Power System	8727 kW
Fuel Cell	4467 kW
Electrolyzer	4262 kW
Hydrogen Storage	706021 kWh

Table 18 Sizes of components - LSPS=0

From an economical point of view the LCOE is equal to 398.25 €/MWh. This value must be compared to the generation cost for Pantelleria that was 297,9 €/MWh in 2015 (20). The proposed configuration could be competitive in the future with the reduction of the costs of the components. In the next table are summarized the costs of the components.

Component	CAPEX [€]	OPEX [€]	RC [€]	TOT [€]
PV System	13500000	2800000	0	16300000
Wind System	10300000	3870000	0	14170000
Electrolyzer	4140000	2080000	2090000	8310000
Fuel Cell	2830000	1420000	1430000	5680000
H_2 Storage	9960000	2500000	0	12460000
Inverter	866000	467000	460000	1793000

Table 19 Total Costs for LPSP=0

The load can be completely satisfied by a hybrid system. The sizes of the PV and wind power systems are comparable, this confirms the abundance of these two sources in the island. The yearly RES energy output is:

RES Power Production	
PV Power System	18440.04 MWh
Wind Power System	25562.85 MWh

Table 20 RES output - LPSP=0

In the following figure, the energy from RES and the load monthly balance is represented. It is observed that the RES supply is higher than the load.

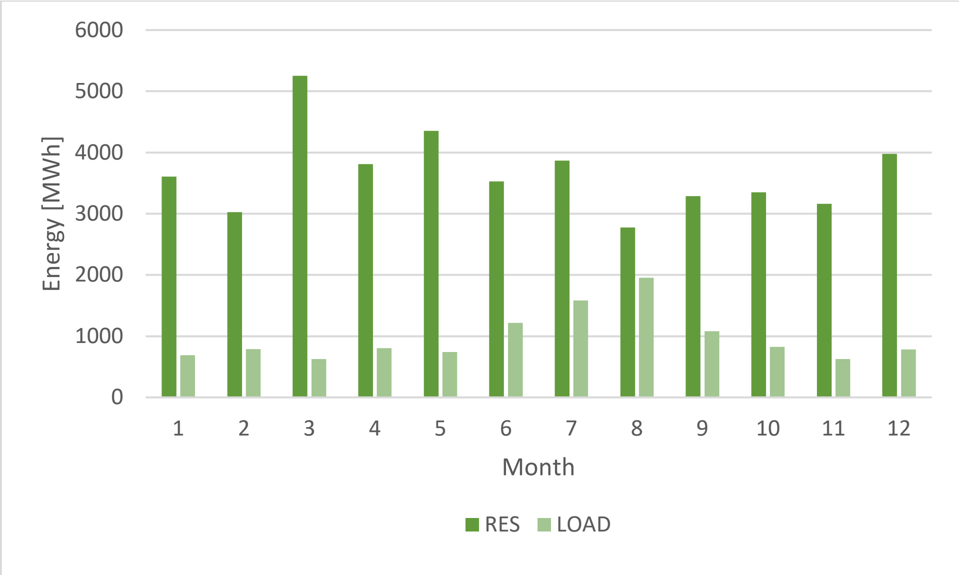

Fig. 31 RES and Load balance

In **Fig. 31** is shown how the load is covered considering the two sources of the systems. The RES provides the highest amount of energy to the demand compared to the fuel cell. The overall distribution follows a seasonal variation.

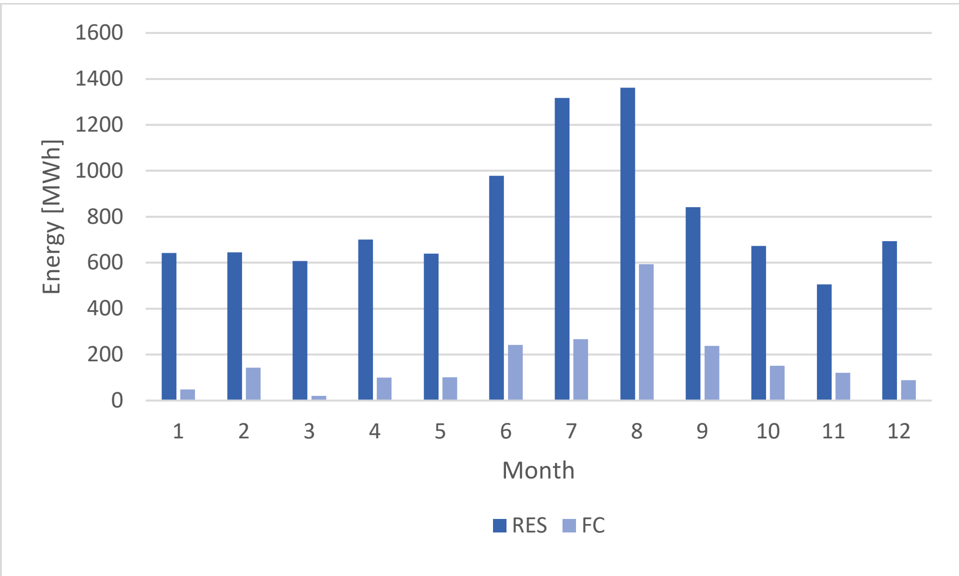

Fig. 32 Load supply distribution

The energy produced by the RES,that is not used from the load, can be stored with the use of the electrolyte or curtailed. From **Fig. 32**, most of the surplus of energy is curtailed, except for two months. This is due to the low difference between the load and the RES supply.

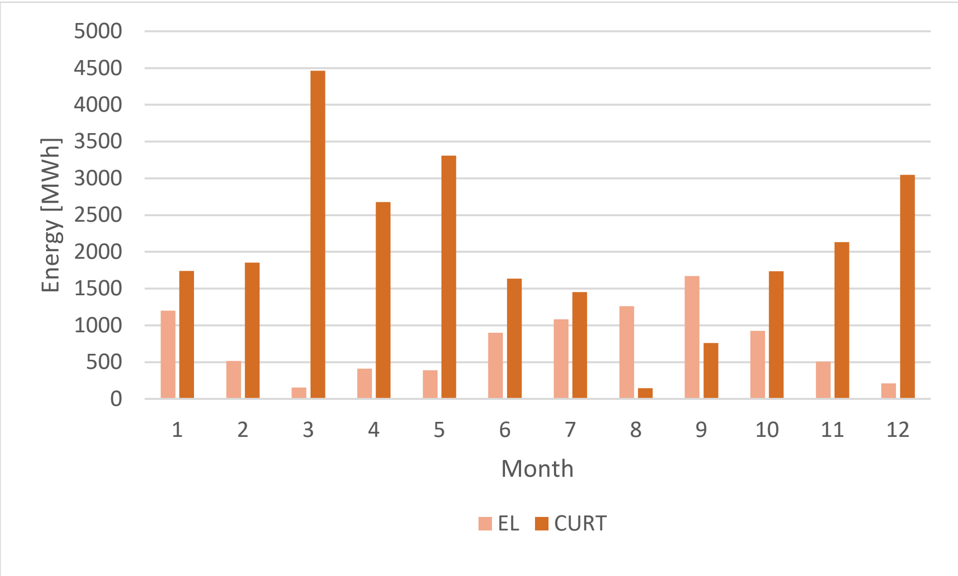

Fig. 33 Surplus energy distribution

In **Fig. 33** the annual variation of the energy contained in the tank is shown. This trend is in accordance with the functioning of the fuel cell, which mostly works during summer. In the rest of the year the maximum energy is reached and the most of the energy is curtailed.

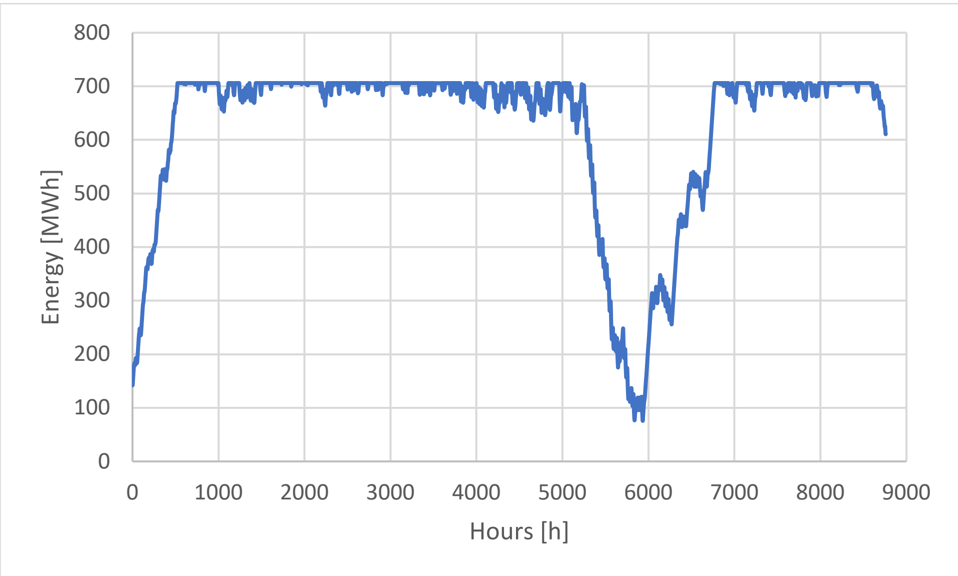

Fig. 34 Energy stored in the hydrogen storage

CASE 2: LPSP=0.5

Setting the LPSP=0.5, the optimized sizes are summarized below:

Residential Load - Hydrogen

PV Power System	8790 kW
Wind Power System	8910 kW
Fuel Cell	2500 kW
Electrolyzer	3930 kW
Hydrogen Storage	625770 kWh

Table 21 Sizes of components - LSPS=0.5

The LCOE with LPSP=0.5 is equal to 370 €/MWh. Compared to the previous case, it assumes a lower value. It is not enough low to be competitive with the current cost of generation. In **Table 22** the costs of the system are sumarized.

Component	CAPEX [€]	OPEX [€]	RC [€]	TOT [€]
PV System	12800000	2650000	0	15450000
Wind System	10500000	3940000	0	14440000
Electrolyzer	3920000	1970000	1980000	7870000
Fuel Cell	1880000	947000	950000	3777000
H_2 Storage	8830000	2210000	0	11040000
Inverter	820000	442000	436000	1698000

Table 22 Total Costs for LPSP=0.5

Comparing **Table 20** and **Table 23**, a sligthly difference between the two cases can be noted. Changing the LPSP value, the optimal configuration has the same RES sizes.

RES Power Production

PV Power System	17462.61 MWh
Wind Power System	25853.34 MWh

Table 23 RES output - LPSP=0.5

Therefore, also the energy balance, between RES and load, follows the same trend of the LPSP=0 case.

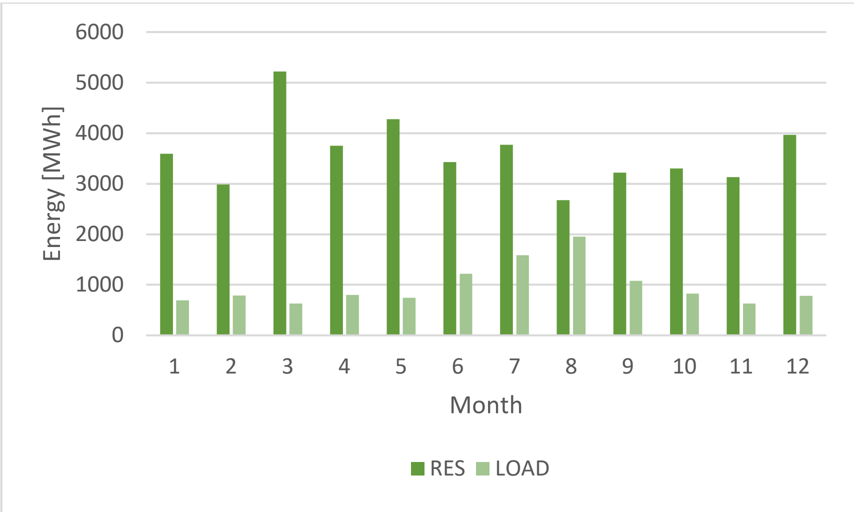

Fig. 35 RES and Load balance

The load is covered by RES and fuel cell. A seasonal variation can be observed for both of them. In particular, the load is satisfyed mostly by the RES.

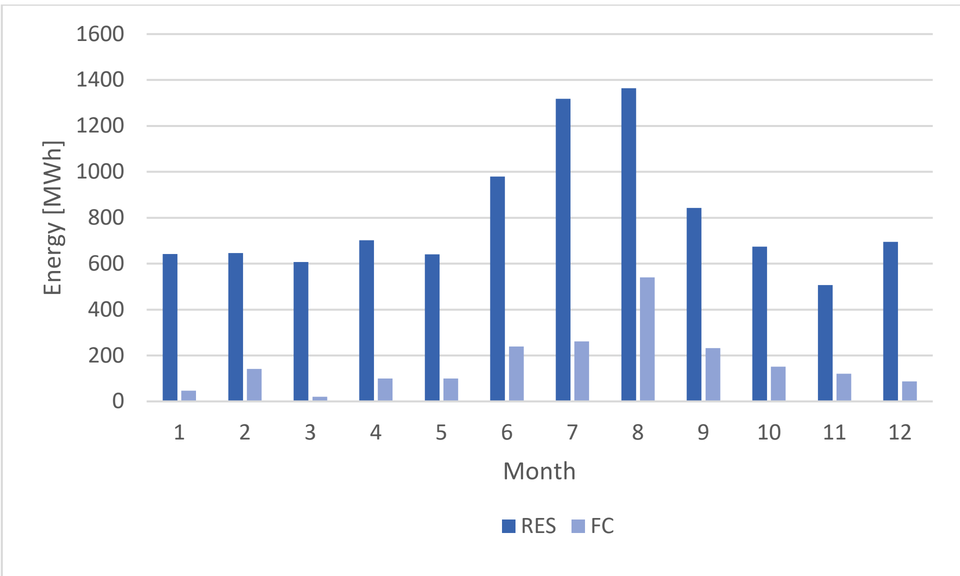

Fig. 36 Load supply distribution

The excess of RES energy is mostly curtailed, while a lower fraction is saved for a later use. At the end of the summer season, the energy stored is higher than the curtailed share, because the load is higher and the fuel celli s exploited more frequently.

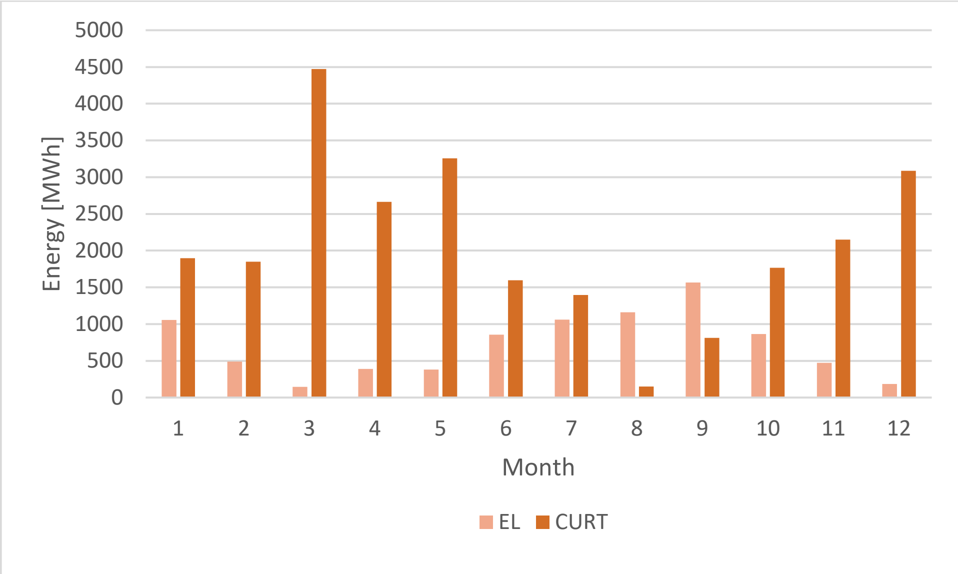

Fig. 37 Surplus energy distribution

The previous trend is verified by the energy stored in the tank. In fact, it drops down during this period of time. In the rest of the year, the energy produced by RES is curtailed and the energy contained in the storage is nearly always at its maximum level.

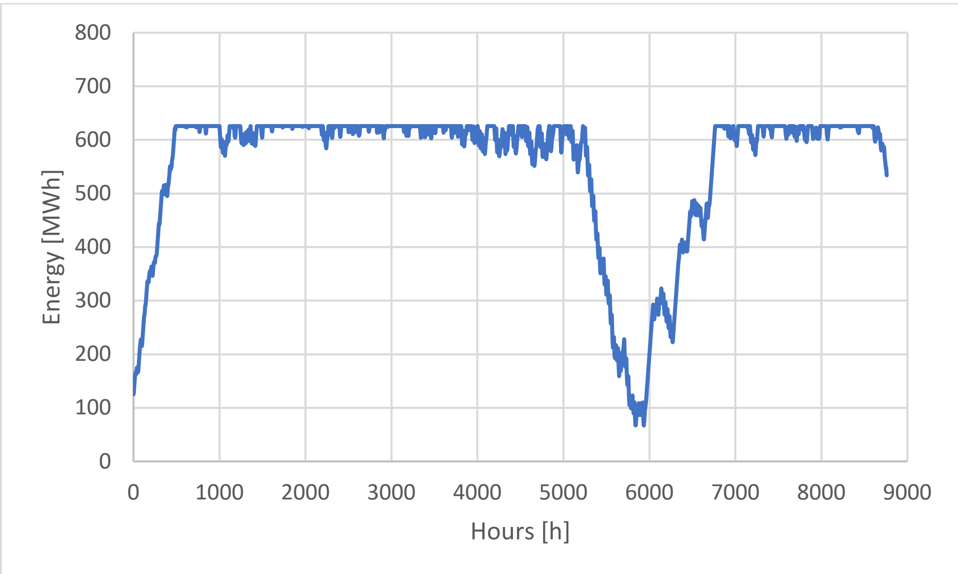

Fig. 38 Energy stored in the hydrogen storage

7.4.2 Residential Load – Hydrogen and Battery

CASE 1: LPSP=0

In the optimized configuration, when LPSP=0, the size of the battery is equal to zero. Therefore, the first case of the previous configuration is obtained. Changing the value of LPSP, a new optimization process is carried out.

CASE 2: LPSP=0.5

Considering a LPSP=0.5, the optimized system is equal to:

Residential Load – Hydrogen/Battery	
PV Power System	8780 kW
Wind Power System	8890 kW
Fuel Cell	2530 kW
Electrolyzer	3920 kW
Hydrogen Storage	617000 kWh
Battery	119 kWh

Table 24 Sizes of components - LSPS=0.5

In this configuration the LCOE is equal to 369.9 €/MWh that is lower than the previous case, but is still higher to be competitive with 297,9 €/MWh.

Component	CAPEX [€]	OPEX [€]	RC [€]	TOT [€]
PV System	12800000	2650000	0	15450000
Wind System	10400000	3940000	0	14340000
Electrolyzer	3920000	1970000	1980000	7870000
Fuel Cell	1890000	955000	959000	3804000

H_2 Storage	8700000	2190000	0	10890000
Inverter	819000	442000	435000	1696000
Battery	65300	14900	40500	120700

Table 25 Total Costs for LPSP=0.5

Even in this case the RES production is higher, but the energy balance is supported by a battery. Moreover, not all the load is covered continously. The RES production is shown in **Table 26**.

RES Power Production	
PV Power System	17442.74 MWh
Wind Power System	25853.34 MWh

Table 26 RES output - LPSP=0.5

Analysing the energy balance, it is possible to observe that the RES production is higher than the load. In particular, the load follows a seasonal variation.

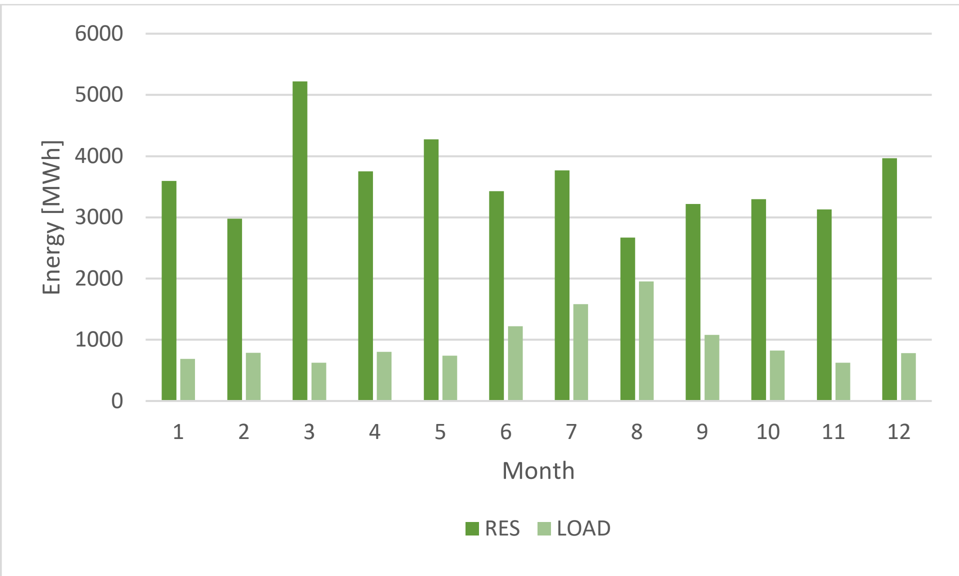

Fig. 39 RES and load balance

In this configuration, the load is covered by the RES, the fuel cell and the battery. Considering the size of the battery, its contribution is negligible compared to the other two sources. The load is firstly met by RES, followed by fuel cell and the battery.

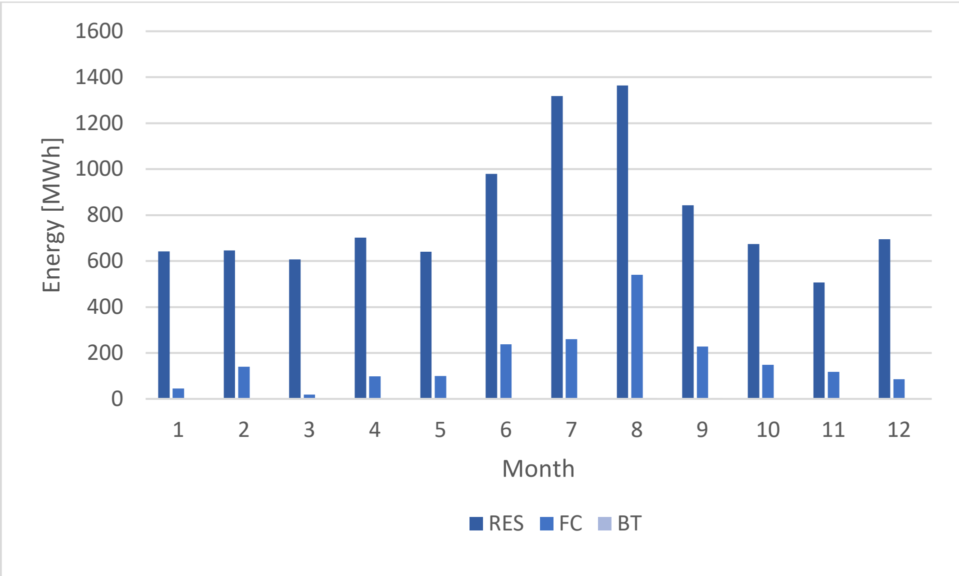

Fig. 40 Load supply distribution

The surplus of energy from RES can be stored in the battery, curtailed or saved for later with an electrolyte. The amount of energy stored in the battery is negligible

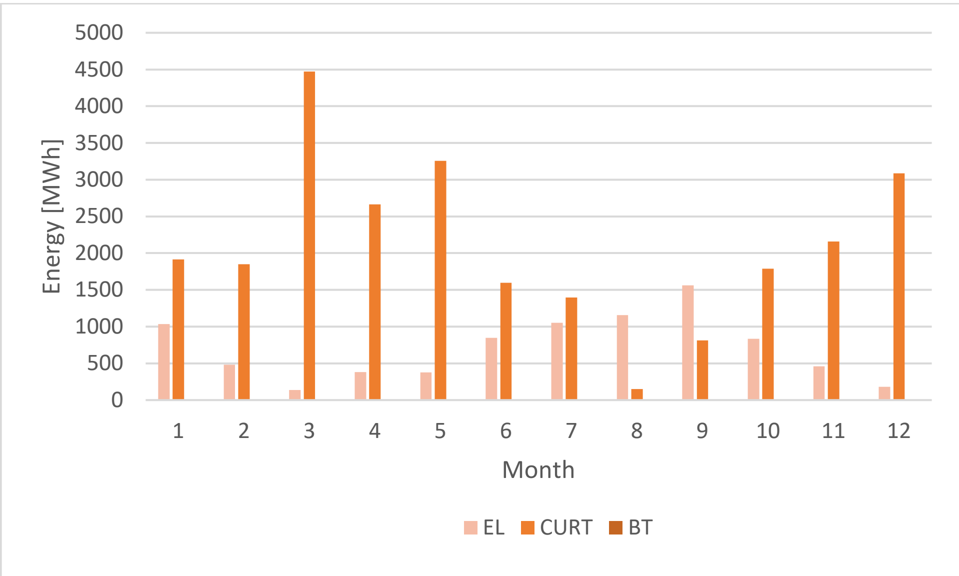

Fig. 41 Surplus energy distribution

The energy stored in the hydrogen tank reaches 600 MWh for most of the year, while during summer the energy drops.

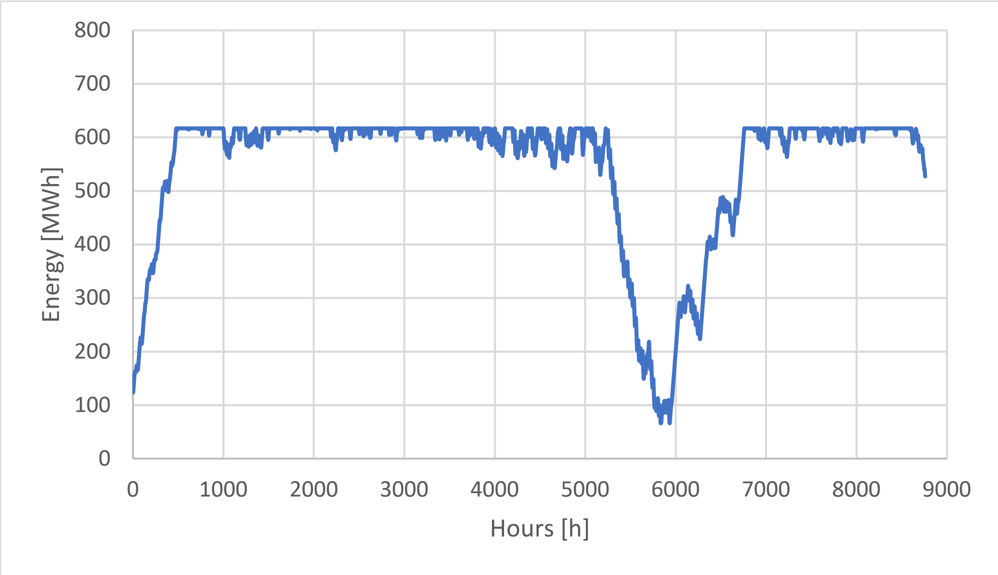

Fig. 42 Energy stored in the hydrogen storage

7.4.3 Mobility Load – Hydrogen

The sizing procedure is carried out with the use of excel. The input data considered are the hydrogen demand for the public transport and the PV output power. The size of the PV is evaluated using a given capacity factor (23%), while the size of the electrolyzer is obtained considering a fixed efficiency of 70%. The sizing of the hydrogen refueling station is obtained considering to satisfy the total hydrogen demand.

The mobility load is covered with the following system:

Mobility Load – Hydrogen/Battery

PV Power System	320 kW
Electrolyzer	264 kW
Hydrogen Storage	1744 kg

Table 27 Sizes of components

The costs of the system are given in **Table 28**.

Component	CAPEX [€]	OPEX [€]	RC [€]	TOT [€]
PV System	465065.6	96510.42	0	561576
Electrolyzer	678328.2	340967.4	343151.3	1362447
H_2 Storage	819680	206009.5	0	1025690
Inverter	29865.6	16085.07	793.1839	46743.85

Table 28 Total Costs

According to Minutillo et al. (47), the LCOH for a grid connected refueling station, able to supply 50 kg/day of hydrogen, is 12.48 €/kg. The evaluated LCOH is equal to 17.88 €/kg, which makes it not competitive. It must also be taken into account that the result is obtained from a preliminary design and it is not optimized from an economic point of view.

CHAPTER 8

SENSITIVITY ANALYSIS

The sensitivity analysis is carried out changing the lifetime of the plant. In particular the lifetime considered are 10, 15, 20, 25 and 30 years. A change of this parameter affects the solution from an economic point of view. The three configurations are considered and the parameters evaluated are the NPC, LCOE and LCOH.

8.1 Residential Load – Hydrogen

CASE 1: LPSP=0

Lifetime	10	15	20	25	30
NPC [€]	51072000	55771000	58756000	61319000	67666000
LCOE [€/MWh]	561.7	455.5	398.9	367.6	371.4

Table 29 Sensitivity Analysis - LPSP=0

CASE 2: LPSP=0.5

Lifetime	10	15	20	25	30
NPC [€]	47409000	51436000	54256000	56751000	62978000
LCOE [€/MWh]	524	422.2	370.3	341.9	347.4

Table 30 Sensitivity Analysis - LPSP=0.5

8.2 Residential Load – Hydrogen and Battery

CASE 1: LPSP=0

Lifetime	10	15	20	25	30
NPC [€]	49799000	55663000	58684000	61335000	67788000
LCOE [€/MWh]	547.7	454.6	398.5	367.7	372.1

Table 31 Sensitivity Analysis - LPSP=0

CASE 2: LPSP=0.5

Lifetime	10	15	20	25	30
NPC [€]	473364000	51439000	54398000	56830000	62718000
LCOE [€/MWh]	523.5	422.19	371.2	342.4	345.9

Table 32 Sensitivity Analysis - LPSP=0.5

8.3 Mobility Load – Hydrogen

Lifetime	10	15	20	25	30
NPC [€]	2542736	2796958	2996456	3153991	3323467
LCOE [€/kg]	24.6	20.1	17.88	16.6	16.03

Table 33 Sensitivity Analysis

The NPC considers both the initial investment cost and the cost sustained during the lifetime of the system, therefore an increasing NPC with the lifetime is expected. In particular, its value is affected by the electrolyzer and fuel cell costs, because they must be replaced frequently as compared to the other components. Another reasoning must be done for the LCOE and LCOH. These two parameters are function of the NPC, therefore a rise is expected, but they are also function of the power and hydrogen delivered to supply the demand, that increase with the lifetime. Precisely for this reason, LCOE and LCOH do not follow a increasing or a decreasing trend.

CHAPTER 9

ENVIRONMENTAL ANALYSIS

The main benefit of the use of hydrogen, is the reduction of CO_2 emissions. In this work, the CO_2 avoided emissions come from the use of RES and a storage of hydrogen to supply both residential and transport loads.

9.1 CO_2 and Mobility

The evaluation of the CO_2 that is not released in the atmosphere, the CO_2 emitted per liter of fuel, in this case diesel, and the amount of fuel used all over the year are needed. According to (48) the CO_2 emission factor f_{em} is equal to 3.13 kg_{CO2}/l_{diesel}, while the specific fuel consumption c_{fuel} is 0.35 l_{diesel}/km. Therefore:

$$CO_2 = PL\, f_{em}\, c_{fuel}$$

Where PL is the length of the path. The annual fuel consumption and the CO_2 avoided are summarized in the following table.

	Diesel [l/day]	CO_2 [kg/day]	Diesel [l/year]	CO_2 [kg/year]
Pantelleria – Tracino – Pantelleria	63.7	199.4	23250.5	72774.1
Pantelleria – Rekale – Pantelleria	78.4	245.4	28616	89568.1

Table 34 Emissions avoided - Mobility

The total amount of CO_2 avoided is equal to 162342.2 kg_{CO2} per year.

9.2 CO_2 and Energy Production

The CO2 emission to supply the residential load can be evaluated considering that Pantelleria produces the energy required with the use of 8 diesel generators.

The total amount of CO2 produced can be evaluated with the total residential load and the CO2 emitted per MWh produced, taken from (49), is equal to 1345.45 kg_{CO2}/MWh. Therefore:

$$CO_{2,RESIDENTIAL} = LOAD\, E_{CO2/MWh}$$

The total amount of CO_2 produced, considering the annual load equal to 11719 MWh/y, is 15767,32 ton_{CO2}/y.

CHAPTER 10

CONCLUSIONS AND FUTURE PERSPECTIVE

The growing concern about climate change has captured the global interest in the energy sector. In particular, the main challenge is represented by the energy transition, in which hydrogen can play a key role.

Hydrogen represents a viable solution to mitigate climate change because it is a multi-purpose energy carrier and this work wants to demonstrate its potential.

In particular, two different configurations are analyzed: a Power-to-Power and a Power-to-Gas system. Both configurations produce hydrogen starting from the energy coming from RES. In the former case, hydrogen is stored in a tank to be converted in electricity when required. In the latter case, hydrogen is exploited directly as a fuel, to refueling a fuel cell vehicle. This can be an interesting choice for off-grid areas, like islands, because this solution guarantees independence from fossil fuels. In fact, the purchase and transportation of fossil fuel to these areas is economically and environmentally unsustainable.

The study is focused on Pantelleria island, which is not connected to the national electricity grid. In the first part the loads (residential and mobility), the solar potential and the wind potential were evaluated. These values were used as input data to size the P2P system and the P2G system.

The sizing of the P2P configuration was carried out using the PSO optimization technique, able to size each component while minimizing the LCOE. Setting different values of LPSP, the sizes of RES systems can be considered stable at 9 MW. The P2G system has been sized thinking of being able to fully cover the load for mobility, obtaining a PV system of 320 kW.

Two P2P configurations have been studied: one that involves the use of hydrogen only, while the other a hydrogen-battery combination. From an economic point of view, considering a lifetime of 20 years, the best solution is the one that uses only hydrogen, obtaining an LCOE of 398.25 €/MWh. This value is not competitive considering that the current power generation price is equal to 297.9 €/MWh. In the case of the P2G system, a configuration with an LCOH of 17.88 €/kg was obtained, that is higher than 12.48 €/kg, that is the result obtained for a micro refueling station connected to the grid.

In both cases, one of the greatest benefits is represented by the avoided CO_2 emissions which are equal to 15767.32 ton_{CO2}/y and 162342.2 kg_{CO2}/y in the case of P2P and P2G respectively.

P2P and P2G systems, thanks to future technological developments, will be more competitive from an economic point of view, as their diffusion on the market will lead to a reduction in prices. In addition, they are useful technologies to face the energy transition.

References

1. **United Nations Framework Convention on Climate Change.** Paris Agreement. [Online] 2015. https://unfccc.int/process-and-meetings/the-paris-agreement/the-paris-agreement.

2. **Masson-Delmotte, V., P. Zhai, H.-O. Pörtner, D. Roberts, J. Skea, P.R. Shukla,A. Pirani, W. Moufouma-Okia, C. Péan, R. Pidcock, S. Connors, J.B.R. Matthews, Y. Chen, X. Zhou, M.I. Gomis, E. Lonnoy, T. Maycock,M. Tignor, and T. Waterfield (eds.).** Global Warming of 1.5°C. An IPCC Special Report on the impacts of global warming of 1.5°C above pre-industrial levels and related global greenhouse gas emission pathways, in the context of strengthening the global response to the threat of climate change,. *IPCC.* [Online] 2018. https://www.ipcc.ch/sr15/.

3. *The value of hydrogen and carbon capture, storage and utilisation in decarbonising energy: Insights from integrated value chain optimisation.* **Christopher J. Quarton, Sheila Samsatli.** 113936, 2020, Applied Energy, Vol. 257. ISSN 0306-2619.

4. **World Energy Outlook 2020. *Interantional Energy Agency.* [Online] https://www.iea.org/reports/world-energy-outlook-2020?mode=overview.**

5. A European Green Deal. *European Commission.* [Online] 2019. https://ec.europa.eu/info/strategy/priorities-2019-2024/european-green-deal_en#documents.

6. *Energy System Modelling of Carbon-Neutral Hydrogen as an Enabler of Sectoral Integration within a Decarbonization Pathway.* Evangelopoulou S, De Vita A, Zazias G, Capros P. 13, 2019, Vol. 12.

7. IEA. World Energy Outlook 2019. Paris : IEA, 2019.

8. World Energy Transitions Outlook: 1.5°C Pathway. *IRENA.* [Online] 2021. www.irena.org/publications. 978-92-9260-334-2.

9. Renewable energy statistics. *Eurostat - Statistics Explained.* [Online] https://ec.europa.eu/eurostat/statistics-explained/index.php?title=Renewable_energy_statistics.

10. Electricity and heat statistics. *Eurostat - Statistics Explained.* [Online] https://ec.europa.eu/eurostat/statistics-explained/index.php?title=Electricity_and_heat_statistics.

11. Kyrre Sundseth, Kjetil Midthun, Mats Aarlott, Adrian Werner,Daniele Consoli, Martina Ciani Bassetti, Stella Chatzigavriil, Roberta Giuliano, Ilaria Schiavi, Manuel Lai, Bernhard Kvaal, Alberto Carpita. *Deliverable D2.1 - Analysis of the economic and regulatory framework of the technological demonstrators.* 2018.

12. *Power-to-X: Between Electricity Storage, e-Production, and Demand Side Management.* Burre, Jannik, et al. 1-2, 2020, Vol. 92. 0009-286X.

13. *The role of hydrogen in low carbon energy futures–A review of existing perspectives.* Emma S. Hanley, JP Deane, BP Ó Gallachóir. 2018, Vol. 82, p. 3027-3045. 1364-0321.

14. *Power-to-gas for injection into the gas grid: What can we learn from real-life projects, economic assessments and systems modelling?* Christopher J. Quarton, Sheila Samsatli. 2018, Vol. 98, p. 302-316. 1364-0321.

15. *The role of renewable hydrogen and inter-seasonal storage in decarbonising heat – Comprehensive optimisation of future renewable energy value chains.* Sheila Samsatli, Nouri J. Samsatli,. 2019, Vol. 233–234, p. 854-893. 0306-2619.

16. *A review of energy storage types, applications and recent developments.* S. Koohi-Fayegh, M.A. Rosen. 2020, Journal of Energy Storage, Vol. 27. 2352-152X.

17. *Handbook On Battery Energy Storage System.* Kim, Dae Kyeong, Susumu Yoneoka, Ali Zain Banatwala, and Yu-Tack Kim. 2018. 978-92-9261-471-3.

18. *GeoDemo - Istat.* [Online] http://demo.istat.it/index.php.

19. Geografia Pantelleria. [Online] https://www.ilovepantelleria.it/geografia.html.

20. Clean Energy Transition Agenda: Pantelleria. *Clean energy for EU islands.* [Online] 2020. https://www.euislands.eu/index.php/document/clean-energy-transition-agenda-pantelleria.

21. *Hydrogen Production from Sea Wave for Alternative Energy Vehicles for Public Transport in Trapani (Italy).* Vincenzo Franzitta, Domenico Curto, Davide Rao and Alessia Viola. 10, 2016, Vol. 9.

22. L'ATLANTE GEOGRAFICO DELLE RINNOVABILI. *GSE - Gestione dei Sistemi Energetici.* [Online] https://www.gse.it/dati-e-scenari/atlaimpianti.

23. Spertino, F. Photovoltaic Power Systems (short handbook). 2016.

24. Notes from "energetica and fonti rinnovabili" course.

25. HOMER Pro 3.14. *HOMER Energy.* [Online] https://www.homerenergy.com/products/pro/docs/latest/how_homer_calculates_the_pv_array_power_output.html.

26. *Optimal design of stand-alone solutions based on RES + hydrogen storage feeding off-grid communities.* Paolo Marocco, Domenico Ferrero , Andrea Lanzini , Massimo Santarelli. 2021, Vol. 238. 0196-8904.

27. *Dynamic modeling of a photovoltaic hydrogen fuel cell hybrid system.* J.J. Hwang, L.K. Lai, W. Wub, W.R. Chang. 23, 2009, International Journal of Hydrogen Energy, Vol. 34.

28. Spertino, Filippo. WIND POWER SYSTEMS (short handbook). 2016.

29. John A. Duffie, William A. Beckman, Nathan Blair. *Solar Engineering of Thermal Processes, Photovoltaics and Wind.* Fifth Edition. s.l. : John Wiley & Sons, Inc., 2020. 9781119540328.

30. J. F. Manwell, J. G. McGowan, A. L. Rogers. *Wind Energy Explained: Theory, Design and Application.* s.l. : John Wiley & Sons, Ltd, 2009. 9781119994367.

31. ***Different Models for Forecasting Wind Power Generation: Case Study.*** **David Barbosa de Alencar, Carolina deMattos Affonso, Roberto Célio Limão de Oliveira,Jorge Laureano Moya Rodríguez, Jandecy Cabral Leite, José Carlos Reston Filho. 2017, Vol. 10.**

32. ***WES - Wind Energy Solutions.*** **[Online] https://windenergysolutions.nl/wes/windturbine-wes-100/#toggle-id-1.**

33. ***Hydrogen production by PEM water electrolysis – A review.*** **S. Shiva Kumar, V. Himabindu. 2019, Materials Science for Energy Technologies,, Vol. 2.**

34. ***Control of Fuel Cell Breathing: Initial Results on the Oxygen Starvation Problem.*** **Jay T. Pukrushpan, Anna G. Stefanopoulou, Huei Peng. 2021.**

35. ***Hydrogen Fueling Stations Infrastructure.*** **Qin N., Brooker P., Srinivasan S. Cocoa, FL, USA : s.n., 2017.**

36. ***Siting and sizing of the hydrogen refueling stations with on-site water electrolysis hydrogen production based on robust regret.*** **Guoming Yang, Yuewen Jiang. s.l. : Wiley, 2020, Int J Energy Res., Vol. 44.**

37. Michael Dolman, Martin Gallmetzer. ***Operators' guide to fuel cell bus deployment - Deliverable D1.2.*** **2018.**

38. ***Optimal Design of Stand-alone Solutions Based on RES hydrogen Storage Feeding Off-grid Communities.*** **Marocco, Paolo, Domenico Ferrero, Andrea Lanzini, and Massimo Santarelli. 2021, Energy Conversion and Management, Vol. 238. 0196-8904.**

39. ***Energy Saving in Public Transport Using Renewable Energy.*** **Franzitta, V., et al. 1, 2017, Vol. 9.**

40. Photovoltaic Geographical Information System (PVGIS). [Online] https://ec.europa.eu/jrc/en/pvgis.

41. John A. Duffie, William A. Beckman, Nathan Blair. ***Solar Engineering of Thermal Processes, Photovoltaics and Wind.*** **s.l. : Wiley, 2020. 978-1-119-54028-1.**

42. ***Potential, optimization and sensitivity analysis of photovoltaic-diesel-battery hybrid energy system for rural electrification in Algeria.*** **F. Fodhil, A. Hamidat, O. Nadjemi. 2019, Vol. 169. 0360-5442.**

43. ***Design optimization of grid-connected PV-Hydrogen for energy prosumers considering sector-coupling paradigm: Case study of a university building in Algeria.*** **Charafeddine Mokhtara, Belkhir Negrou, Noureddine Settou, Abdessalem Bouferrouk, Yufeng Yao. 75, 2021, Vol. 46. 0360-3199.**

44. **Paolo Marocco, Domenico Ferrero, Marta Gandiglio, Massimo Santarelli, Villy Biltoft, Daniele Consoli, Martina Ciani Bassetti, Ilaria Rosso, Lorenzo Cantone, Olivia Rigovacca, Stella Chatzigavriil, Denis Thomas, Stefan Knauf, Ilaria Schiavi et al.** ***"Remote area Energy supply with Multiple Options for integrated hydrogen-based TEchnologies", Deliverable number 2.2.*** **2019.**

45. ***Optimal design of stand-alone solutions based on RES + hydrogen storage feeding off-grid communities.*** **Paolo Marocco, Domenico Ferrero, Andrea Lanzini, Massimo Santarelli. 2021, Vol. 238. 0196-8904.**

46. ***A study of the techno-economic feasibility of H2-based energy storage systems in remote areas.*** **P. Marocco, D. Ferrero, M. Gandiglio, M.M. Ortiz, K. Sundseth, A. Lanzini, M. Santarelli. 2020, Vol. 211. 0196-8904.**

47. ***Analyzing the levelized cost of hydrogen in refueling stations with on-site hydrogen production via water electrolysis in the Italian scenario.*** **M. Minutillo, A. Perna, A. Forcina, S. Di Micco, E. Jannelli. 2021, Vol. 46. 0360-3199.**

48. ***Prospects and impediments for hydrogen fuel cell buses.*** **A. Ajanovic, A. Glatt, R. Haas. 2021, Vol. 235. 0360-5442.**

49. ***Renewable electricity generation for off grid remote communities; Life Cycle Assessment Study in Alaska, USA.*** **Christopher S. McCallum, Narendran Kumar, Robin Curry, Katherine McBride, John Doran. 2021, Vol. 299. 0306-2619.**

50. ***Thermoeconomic modeling of a completely autonomous, zero-emission photovoltaic system with hydrogen storage for residential applications.***

Alexandros Arsalis, Andreas N. Alexandrou, George E. Georghiou. Renewable Energy, Vol. 126, p. 354-369. 0960-1481.

51. ***Feasibility of a standalone photovoltaic/battery system with hydrogen production.*** **Hanane Hassani, Faika Zaouche, Djamila Rekioua, Saloua Belaid, Toufik Rekioua, Seddik Bacha. 2020, Journal of Energy Storage, Vol. 31. 2352-152X.**

52. ***Energy Management for Stand Alone Hybrid Photovoltaic – PEM Fuel Cells Systems.*** **Mutomboa, Ntumba Marc-Alain e Freddie L. Inambaob, Remy Tiakoc and Samuel A. O. Ilupejud. 19, 2017, International Journal of Applied Engineering Research, Vol. 12. 0973-4562.**

53. ***Techno-economic analysis of a hybrid system to power a mine in an off-grid area in Ghana,.*** **Martin Ansong, Lena D. Mensah, Muyiwa S. Adaramola. 2017, Sustainable Energy Technologies and Assessments, Vol. 23, p. 48-56. 2213-1388.**

54. ***Technical-economic analysis of a hydrogen production facility for power-to-gas and hydrogen mobility under different renewable sources in Southern Italy.*** **Petronilla Fragiacomo, Matteo Genovese. 2020, Vol. 223. 0196-8904.**

55. ***Techno-economic implications of the electrolyser technology and size for power-to-gas systems.*** **David Parra, Martin K. Patel. 2016, Vol. 41. 0360-3199.**

56. ***State-of-the art CAPEX data for water electrolysers, and their impact on renewable hydrogen price settings.*** **Proost, Joris. 2019, Vol. 44. 0360-3199.**

57. ***Study on early business cases for H2 in energy storage and more broadly power to H2 applications.*** **Hinicio, Tractebel and. 2017.**

58. ***Microgrid sizing with combined evolutionary algorithm and MILP unit commitment.*** **Bei Li, Robin Roche, Abdellatif Miraoui. 2017, Vol. 188. 0306-2619.**

59. ***Integration of sizing and energy management based on economic predictive control for standalone hybrid renewable energy systems.*** **P. Rullo, L. Braccia, P. Luppi, D. Zumoffen, D. Feroldi. 2019, Vol. 140. 0960-1481.**

60. ***Control based on techno-economic optimization of renewable hybrid energy system for stand-alone applications.*** **Juan P. Torreglosa, Pablo García-Triviño, Luis M. Fernández-Ramirez, Francisco Jurado. 2016, Vol. 51. 0957-4174.**

61. ***Thermo-economic analysis of a hydrogen production system by sodium borohydride (NaBH4).*** **M. Rivarolo, O. Improta, L. Magistri, M. Panizza, A. Barbucci. 2018, Vol. 43. 0360-3199.**

Figure Index

Table Index